Shape factors and cross-sectional risk

Andrea Roncoroni, Stefano Galluccio, Paolo Guiotto

Shape factors and cross-sectional risk

Andrea Roncoroni, Stefano Galluccio, Paolo Guiotto

PII: S0165-1889(10)00132-6
DOI: doi:10.1016/j.jedc.2010.06.002
Reference: DYNCON 2432

To appear in: *Journal of Economic Dynamics & Control*

Cite this article as: Andrea Roncoroni, Stefano Galluccio and Paolo Guiotto, Shape factors and cross-sectional risk, *Journal of Economic Dynamics & Control*, doi:10.1016/j.jedc.2010.06.002

Shape Factors and Cross-Sectional Risk

Andrea Roncoroni* ESSEC
Stefano Galluccio BNP Paribas
Paolo Guiotto Università di Padova

Abstract

Galluccio and Roncoroni (2006) empirically demonstrate that cross-sectional data provide relevant information when assessing dynamic risk in fixed income markets. We put forward a theoretical framework supporting that finding based on the notion of "shape factors". We devise an econometric procedure to identify shape factors, propose a dynamic model for the yield curve, develop a corresponding arbitrage pricing theory, derive interest rate pricing formulae, and study the analytical properties exhibited by a finite factor restriction of rate dynamics that is cross-sectionally consistent with a family of exponentially weighed polynomials. We also conduct an empirical analysis of cross-sectional risk affecting US swap, Euro bond, and oil markets. Results support the conclusion whereby shape factors outperform the classical yield (resp. price) factors (i.e., level, slope, and convexity) in explaining the underlying fixed income (resp. commodity) market risk. The methodology can in principle be used for understanding the intertemporal dynamics of any cross-sectional data.

*Corresponding author, Finance Department, ESSEC Business School, Paris-Singapore, Av. Bernard Hirsch B.P. 50105, 95021 Cergy-Pontoise, France. Tel. +33134433239; Fax. +33134433001; e-mail: roncoroni@essec.fr.

Acknowledgements: We would like to thank the participants to the Second Annual Conference on Risk Management organized by the Risk Management Institute (RMI) of the National University of Singapore, and Jonathan Lipsmeyer for valuable comments on an earlier version of the paper. Roncoroni gratefully acknowledges financial support from CERESSEC and the Bruti-Liberati Fundation. This research was finalized while the first author was Visiting at the University of Technology Sydney. We finally wish to thank BNP Paribas for kindly providing data. The usual disclaimers apply.
Key words: Risk Measures, Factor Analysis, Cross-Sectional Analysis, Interest Rates.
JEL Classification: C31, E43, G11.

1 Introduction

The random behavior of yield curve dynamics is reflected in the market risk underlying interest rate positions. Modeling these dynamics can be a difficult task given the high number of involved rates. This study seeks to identify and hedge against a reduced number of significant factors affecting the evolution of cross-sectional data.

The subject has received a great deal of attention in the last thirty years. All methods share a common preliminary *cross-sectional analysis* aimed at building a term structure matching a limited number of quoted values (Anderson *et al.* (1996) and Nelson and Siegel (1987)). This analysis offers a complete picture of the way the market quotes the time value of money at a given date. However, it provides no information about the evolution of the resulting term structure. Consequently, alternative methodologies have been introduced for the purpose to provide a description of cross-sectional dynamics.

An early strand of literature, referred to as *functional immunization*, assigned specific functional forms to any admissible term structure updating (*e.g.*, parallel shifts in Fisher and Weil (1972), arbitrary variations in Fong and Vasiček (1984), and selected analytical forms in Chambers and Carleton (1988), Prisman and Shores (1988), Barrett *et al.* (1995), Phoa and Shearer (1997), and Rodrigues De Almeida *et al.* (1998)) and provided selection criteria for bond portfolios to make them financially insensitive to these deformations. The approach exhibits the remarkable feature of accounting for full information about the cross-section. Unfortunately, it provides no statistical support for the selected deformations, which are usually chosen on the basis of qualitative considerations. This fact may hamper the effectiveness of the corresponding hedging strategies.

Another branch of literature focuses on the identification of underlying driving *factors*. These factors may be set as a number of selected cross-sectional points (*e.g.*, optimal key rates in Elton *et al.* (1990) and affine yield factors in Duffie and Kan (1996)), or suitable linear combinations of cross-sectional points usually determined by means of statistical analysis (*e.g.*, principal components in Litterman and Scheinkman (1991) and affine Gaussian factors in Collin-Dufresne *et al.* (2008)). Factors are ranked according to their contribution to the historical market volatility, and the most significant ones are retained as representative risk drivers. The methodology dramatically simplifies the identification of effective risk management strategies. However, and in contrast to the aforementioned immunization approach, it does so irrespectively of the informational content embodied in the typical

shapes displayed by cross-sectional data.

These approaches underline a tension between the 1) *cross-sectional representativeness* of traditional immunization and the 2) *statistical relevance* of existing parsimonious factor-based models driving cross-sectional dynamics. This point leads us to our first theoretical issue which we illustrate in Panel 1.

		Cross-Sectional Representativeness	
		Incomplete	Complete
Statistical Relevance	Unassessed	-	*Functional Immunization*
	Assessed	*Principal Components* *Optimal Key Rate*	?

Panel 1: Trade-off between cross-sectional representativeness and statistical relevance.

Issue 1: Can we resolve the above dilemma and deliver a statistical assessment (and ranking) of all information stemming from cross-sectional analysis?

As a leader of these paradigms, *arbitrage-free modeling* has been widely developed throughout interest rate information systems. The resulting theory aims at providing consistent prices and hedging prescriptions for the vast majority of interest rate securities. Models typically combine a quoted yield curve with factors possessing an acceptable degree of statistical relevance. This fact raises a second theoretical question about the ability to provide a solution to the issue stated above.

Issue 2: Can we build arbitrage-free models driven by factors subsuming a statistical assessment of the information embodied in cross-sectional data?

Inspired by empirical evidence shown in Litterman *et al.* (1991) and Engle and Ng (1993), Galluccio and Roncoroni (2006) provide a positive answer to the first issue above. They first introduce an *empirical measure of risk* accounting for an explicit link between yield curve shapes and volatility.[1] Then, they pursue an extensive empirical study of its performance on representing and managing risk underlying U.S. Treasury Bond portfolios. They finally

[1] This result is tantamount to extending the classical expectation hypothesis that relates yield curve shape to expected bond returns as in Cox *et al.* (1981).

compare the resulting hedging errors to those stemming from the standard strategy of delta hedging against cross-yield principal components.

Based on these empirical findings, we offer a positive answer to the second issue above. First, we provide a *theoretical measure of risk* formalizing the empirical measure proposed earlier. Second, we develop a continuous-time infinite-dimensional *arbitrage-free model* for rate dynamics driven by factors representing this risk. The results of our theoretical analysis of the model include exact arbitrage restrictions to the driving diffusion process, an econometric procedure to identify and measure the underlying factors, interest rate derivative pricing formulae, pricing error bounds for a cross-sectionally consistent model restriction, and additional empirical evidence on interest rate as well as commodity markets. To the best of our knowledge, the model represents the first use of infinite-dimensional models based on empirical evidence.

The paper is organized as follows. Section 2 proposes a theoretical econometric procedure to estimate cross-sectional covariance structures using a functional version of Principal Components Analysis (PCA). Section 3 develops a dynamic theory of shape factors. Section 4 provides a theoretical analysis of dynamic models driven by shape factors. Section 5 develops an empirical analysis of shape factors that complements the comprehensive study in Galluccio and Roncoroni (2006). Section 6 draws conclusions and sheds light on a few issues meriting future research.

2 The Notion of Shape Factors

The problem of decomposing yield curve dynamics into a set of statistically independent risk factors dates back to Steeley (1990) and Litterman and Scheinkman (1991).[2] By performing a PCA on a time series of yield curves, the authors identify the three most relevant risk factors. These factors can be interpreted as 1) a parallel shift, 2) a change in steepness, and 3) a twist in the yield curve shape. Despite the appealing appearance of these factors, they show no explicit dependence on the term structure shape stemming from the cross-sectional analysis. In particular, their *analytical* form remains undefined. This fact may result in an incomplete picture of the cross-sectional risk perceived by the market and embodied in the yield curve shape.

[2] Knez *et al.* (1994) formalize the methodology and provide an empirical investigation in the US money market.

In this section, we introduce a notion of shape factors for interest rate data. In particular, we provide a econometric procedure to detect these factors from cross-sectional data and describe the resulting covariance structure.

2.1 Econometrics of Shape Factors

In general, any cross-section is represented by a function $r(t,x)$, where t denotes the calendar time and x represents the cross-sectional dimension. If this variable is a nonnegative number denoting time-to-maturity, the cross-section is referred to as a "term structure". Examples are the instantaneous forward rate curve, the discount function, the forward price curve for a commodity, and the Black-Scholes implied volatility over a set of maturities for a given strike price.

We assume that all cross-sections $r:[0,\infty)\mapsto\mathbb{R}$ in a given market are represented by elements in the linear space $\mathbb{H}_n$ spanned by a finite orthonormal system of functions

$$\Psi_n=\{\psi_i:[0,\infty)\ni x\mapsto\psi_i(x)\in\mathbb{R},i=1,...,n\}$$

with respect to an inner product $\langle\cdot,\cdot\rangle_{\mathbb{H}_n}$. In view of what will be reported in the theoretical analysis detailed in section 3, the class Ψ_n should be extendable to an infinite orthonormal complete system $\Psi=\{\psi_1,...\}$ spanning a Hilbert space $\mathbb{H}$.[3] The time t cross-section $r(t)=\{r(t,x),x\geq 0\}$ is thus a linear combination of the form $a_1(t)\psi_1(x)+...+a_n(t)\psi_n(x)$. Basis functions $\psi_1,...,\psi_n$ are selected to best represent the basis shapes prevailing in the market under investigation, and each coefficient $a_i(t)$ represents the orthogonal projection of the time t cross-section $r(t)$ on the one-dimensional space spanned by the corresponding shape ψ_i. Consequently, the cross-sectional dynamics can be written as follows:

$$r(t,x)=\sum_{i=1}^{n}a_i(t)\psi_i(x)=\sum_{i=1}^{n}\langle r(t),\psi_i\rangle_{\mathbb{H}_n}\psi_i(x).$$

Because $\psi_1,...,\psi_n$ are orthonormal, the map I_n transforming a given cross-section r into the corresponding projection coefficients, namely

$$r\overset{I_n}{\to}(a_1(t),...,a_n(t)):=\mathbf{a}(t),\tag{1}$$

is an isomorphism from $\mathbb{H}_n$ onto $\mathbb{R}^n$, meaning that inner products are preserved:

$$\langle r(t),r(s)\rangle_{\mathbb{H}_n}=\langle\mathbf{a}(t),\mathbf{a}(s)\rangle_{\mathbb{R}^n}.$$

[3] In general, the required extension can be performed through the usual Gram-Schmidt orthonormalization procedure.

Accordingly, the random evolution of a cross-section r in the space $\mathbb{H}_n$ induces corresponding dynamics followed by the vector of coefficients $\mathbf{a}(t)$ in $\mathbb{R}^n$ so that all covariances are preserved. The main consequence is that a PCA on the cross-sectional dynamics in $\mathbb{H}_n$ can be alternatively performed in the Euclidean space $\mathbb{R}^n$.

We remark that the vector $\mathbf{a}(t)$ may be computed by matching a set of observed market points in the cross-section $\left\{r^{\text{obs}}(t,x_j), i=1,...,m\right\}$. If m equals the cardinality n of $\mathbf{a}(t)$, then the system

$$\sum_{i=1}^{n} a_i(t)\psi_i(x_j) = r^{\text{obs}}(t,x_j),\ \forall j=1,\cdots,m,$$

admits a unique solution $\mathbf{a}(t)$, provided its determinant is non-zero. Usually, the number of quoted values exceeds the number of selected shapes and $\mathbf{a}(t)$ must be numerically approximated. A possible solution is provided by the following weighed least-squares minimization program:

$$\min_{\mathbf{a}\in\mathbb{R}^n}\left\{\sum_{j=1}^{m} w_j(t)\left(\sum_{i=1}^{n} a_i(t)\psi_i(x_j) - r^{\text{obs}}(t,x_j)\right)^2\right\}. \tag{2}$$

Each w_j is a loading coefficient, or penalty, for the time t discrepancy between the estimated and the observed point in the cross-section. Loading coefficients represent an important tool for managing the fitting quality at different portions of the observed cross-section. For instance, in the case of interest rate term structures, times to maturity corresponding to liquid and informative securities (*e.g.,* benchmark bonds or swaps) should be assigned relatively large coefficients w_i in order to fit available quoted prices more closely.

By applying the above procedure to observed cross-sections at consecutive dates $0 = t_0,...,t_M = T$, we obtain a time series of coefficient vectors $\mathbf{a}(t_0),...,\mathbf{a}(t_M)$. We assume that this sequence corresponds to a sample from a Gaussian process with constant volatility matrix $\Sigma\in\mathcal{M}(n)$ (*e.g.,* $d\mathbf{a}(t) = \mathbf{b}dt + \Sigma dW(t)$, with $\mathbf{b}\in\mathbb{R}^n$ and W an n-dimensional standard Brownian motion) and define the series of absolute variations by $d\mathbf{a}(t_i) := \mathbf{a}(t_i) - \mathbf{a}(t_{i-1})$. The standard estimator of the covariance matrix $\mathbf{C} = \Sigma\Sigma^{\mathsf{T}}$ is provided by

$$\mathbf{C} = \left(\text{Cov}\left(\widetilde{d\mathbf{a}}_i, \widetilde{d\mathbf{a}}_k\right)\right)_{0\le i,k\le M} \tag{3}$$

where the centered increments per time unit are defined as

$$\widetilde{d\mathbf{a}}(t_i) := \frac{d\mathbf{a}(t_i)}{\sqrt{t_i - t_{i-1}}} - \frac{1}{M}\sum_{k=1}^{M}\frac{d\mathbf{a}(t_k)}{\sqrt{t_k - t_{k-1}}},\ i=1,...,M.$$

It is worth noting that coefficient $\mathbf{b}$ is immaterial for the estimation of the local covariance process of $\mathbf{a}(t)$ (and thus for the covariance operator of r): any drift corresponds to an equivalent measure and the diffusion coefficient remains unchanged.

The process $\widetilde{d\mathbf{a}}$ is a Gaussian random vector with pairwise uncorrelated components with respect to the Cartesian system given by the (normalized) eigenvectors $\mathbf{v}_i$ $(i = 1, \cdots, n)$ of the sample covariance matrix $\mathbf{C}$. After sorting the eigenvalues of $\mathbf{C}$ in decreasing order, we define the diagonal matrix $\Lambda := diag(\lambda_1, ..., \lambda_n)$ and collect the corresponding eigenvectors into a matrix $S = \left(\mathbf{v}^{(1)} \mid \mathbf{v}^{(k)} \mid ... \mid \mathbf{v}^{(n)}\right)$. Since matrix $\mathbf{C}$ is symmetric, all eigenvalues λ_i are positive. Because $\mathbf{C} = S\Lambda S^{\mathsf{T}}$, the volatility matrix is identified by the sample matrix $\mathbf{\Sigma} = S\Lambda^{1/2}$ and the coefficient vector $\mathbf{a}(t)$ can be expressed in the new Cartesian system by rotating its components according to the matrix S, leading to dynamics

$$d[S\mathbf{a}](t) = [S\mathbf{b}]\,dt + \sum_{k=1}^{n} \left\langle d\mathbf{a}(t), \mathbf{v}^{(k)} \right\rangle_{\mathbb{R}^n} \mathbf{v}^{(k)} = [S\mathbf{b}]\,dt + \sum_{k=1}^{n} \left(\sqrt{\lambda_k} dW_k(t)\right) \mathbf{v}^{(k)}. \quad (4)$$

The isometry property in expression (1) ensures that $\mathbf{C}$ represents the sample (average) covariance operator $\mathcal{C}$ of the process followed by the cross-section dynamics in the space $\mathbb{H}_n$. The orthogonal matrix S induces an orthonormal transformation $\mathcal{S}$ in $\mathbb{H}_n$ mapping the initial system $\{\psi_k\}_{k=1}^n$ into the one collecting the eigenmodes of the covariance operator of r in $\mathbb{H}_n$. Each eigenmode f_k can be computed as the counterimage of eigenvector $\mathbf{v}^{(k)}$ according to the mapping I_n, that is

$$f_k(x) = \left[I_n^{-1}\mathbf{v}^{(k)}\right](x) = \sum_{i=1}^{n} \mathbf{v}_i^{(k)} \psi_i(x). \quad (5)$$

By using the definition of cross-section $r(t) = \sum_{i=1}^{n} a_i(t)\,\psi_i$, equation (4) for the rotated dynamics, and expression (5) for the eigenmodes, the drift-compensated cross-section evolution under the new basis $\{f_k\}_{k=1,...,n}$ can be written as

$$d\overline{r}(t, x) = \sum_{k=1}^{n} \sqrt{\lambda_k} f_k(x)\, dW_k(t).$$

Panel 2 summarizes the identification procedure described above.

$$\begin{array}{ccc} \mathbb{H}_n & & \mathbb{R}^n \\ \left(\left\{\langle r(t), \psi_k\rangle_{\mathbb{H}_n}\right\}_{1\le k\le n}, \{\psi_k\}\right) & \xrightarrow{I_n} & \left(\mathbf{a}(t), \{\mathbf{e}^{(k)}\}_{k=1}^n\right) \\ \downarrow \mathcal{S} & & \downarrow S \\ \left(\left\{\langle r(t), f_k\rangle_{\mathbb{H}_n}\right\}_{1\le k\le n}, \{f_k\}\right) & \xleftarrow{I_n^{-1}} & \left([S\mathbf{a}](t), \{\mathbf{v}^{(k)}\}_{k=1}^n\right) \end{array}$$

Panel 2: Shape-factor identification.

2.2 Cross-Shape Covariance Structure

Formula (5) suggests the following definition of shape factor:

Definition 1 (Shape Factor) The k-th shape factor affecting cross-section dynamics with covariance operator $\mathcal{C}$ is the normalized eigenmode corresponding to the k-th largest eigenvalue of $\mathcal{C}$. This can be computed as

$$f_k(x) = \sum_{i=1}^n \mathbf{v}_i^{(k)} \psi_i(x). \tag{6}$$

An easy calculation based on mutual independence among the Brownian motions $W_k(t)$ $(k = 1, ..., n)$ leads to the following closed-form formula for the time T accrued cross-sectional covariance surface expressed in terms of shape factors:

$$C_{[0,T]}(x,y) := \langle r(\cdot, x), r(\cdot, y)\rangle_T = \sum_{k=1}^n \lambda_k f_k(x) f_k(y) T. \tag{7}$$

In particular, the corresponding volatility function is given by $V_{[0,T]}(x) = \sqrt{\sum_{k=1}^n \lambda_k f_k(x)^2 T}$. It is now possible to reproduce a proportion $\alpha \in [0,1]$ of the realized market risk occurred in the period between t and T by a parsimonious number of shape factors.[4] To do so, we define $M := \inf\left\{k : 100 \sum_{i=1}^k \lambda_i / \sum_{i=1}^n \lambda_i \ge \alpha\right\}$ and consider reduced-form dynamics with a truncated diffusion part to the M-th order, namely $\sum_{k=1}^M \sqrt{\lambda_k} f_k(x)\, dW_k(t)$. This completes the econometric procedure to single out shape factors corresponding to a time-series of cross-sectional data in a given market.

[4] Parameter α corresponds to the standard explained volatility cut-off used in Principal Component Analysis.

3 Dynamic Theory of Shape Factors

In the previous section, we have defined a notion of shape factors in agreement with the earlier empirical findings. We now put forward a continuous time interest rate model whose random dynamics are driven by shape factors.

3.1 On the Choice of Model Setting

A benchmark framework in the dynamic theory of interest rates is represented by the Heath, Jarrow and Morton (1992) (HJM). This setting owes its popularity to the remarkable result whereby arbitrage-free models uniquely depend on two quantities. One is the term structure of interest rates prevailing in the market at a given point in time. The other is the cross-factor covariance structure stemming from a risk factor analysis. HJM models combine these two inputs and derive term structure dynamics represented through a continuum of stochastic differential equations. This assumption makes the corresponding dynamic system essentially infinite-dimensional.

There are two alternative approaches to infinite-dimensional stochastic models. A first approach has been introduced by Kennedy (1994) using the theory of random fields (RF) developed in Walsh (1986). The idiosyncratic noise term is described using a Brownian sheet $W(t,x)$. This is a continuous path stochastic process parametrized in both time and space with independent and stationary Gaussian increments. This setting has been adopted by several authors, including Kennedy (1997), Bouchaud *et al.* (1999), Goldstein (2000), Santa Clara and Sornette (2001), Collin-Dufresne and Goldstein (2003), and Kimmel (2004).

Overall the existing literature demonstrates that models based on RF's can be developed for arbitrage pricing purposes. Although they undoubtedly exhibit a set of remarkable analytical properties, these models have a number of qualities that prevent them from appropriately modeling the empirical findings referred to in the introduction about the link between market risk and term structure shapes. First, in a RF model both time t and time-to-maturity x are treated as process parameters in spite of their fundamental difference. Indeed, t is the flow dimension of randomness representing financial risk, whereas x is the cross-sectional dimension fixing market expectations about future quotes. Second, Pang (1999) notes that derivative pricing of exotic derivatives requires a finite-dimensional approximation of any infinite-dimensional model. For this to be the case, driving noises ought to be ranked and selected according to their relative importance in explaining market

risk. Unfortunately, the structure of RF models does not offer any means of performing such a ranking. Finally, all known finite dimensional approximations of RF models are standard HJM specifications. To our knowledge RF models have not proved yet to be superior to any alternative specification within the HJM framework. This fact makes the sophisticated RF theory somehow spurious for practical applications.[5]

A second approach to deal with infinite-dimensional term structure models has been proposed by Musiela (1993). This study is based on the theory of Hilbert-space-valued stochastic differential equations (HSDE) as developed in Da Prato and Zabczyk (1992). The term structure of interest rates is identified with a single point in a functional space and then represented as a superposition of fundamental shapes. Several studies have been pursued in this framework, including Brace and Musiela (1994), Musiela (1995), Filipović (2000), Björk and Christensen (1999), Bayraktar *et al.*(2006), and La Chioma and Piccoli (2007). It is worth noting that all these papers work under the somehow simplified assumption of dynamics driven by a standard n-dimensional Wiener process. Guiotto and Roncoroni (1999) and, independently, Goldys and Musiela (2001) extend this framework to dynamics driven by a function-valued Q-Brownian motion. This process represents the natural extension of a Wiener process in the Hilbert-space $\mathbb{H}$ of term structure shapes as defined in section 2. The setting is further explored in Aihara and Baghi (2005), where arbitrage properties and completeness of a hyperbolic specification are studied in detail.

There are two compelling reasons that make of HSDE an appropriate framework for building models driven by factors related to term structure shapes. First, the nature of both time t and time-to-maturity x is fully accounted for by Q-Brownian motion. This fact allows for the cross-yield covariance surface to be analytically defined as a superposition of statistically uncorrelated yield curve shapes. Equally importantly, the analysis allows for us to rank these shapes in keeping with their explicatory power of the underlying market risk. Second, the HSDE setting is particularly suitable for tackling the consistency problem of finite-dimensional restrictions of the model. In particular, we can assess an exact estimation of the pricing error of cross-sectionally consistent realizations of the infinite-dimensional arbitrage-free model. More importantly, the shape ranking referred to earlier allows us to

[5] For instance, Pang (1999) shows that the yield curve volatility structure can be identified up to a finite number of values. This implies that the covariance function over the whole time to maturity spectrum of the RF has to be recovered by arbitrary interpolation methods. Consequently, the main advantage of RF models, namely the exogenous assignment of a covariance function, is usually lost at the stage of numerical implementation.

devise a procedure to bound the pricing errors to an arbitrarily small extent.

3.2 Arbitrage-Free Dynamics

We now focus our analysis on term structures of instantaneous forward rates. Let $P_T(t)$ denote the time t price of a default-free zero-coupon bond maturing at T. We suppose the discount function $T \mapsto P_T(t)$, $T \geq t$, is continuously differentiable and define the instantaneous forward rate curve $r(t)$ by $r(t,x) := -\partial_x \lg P_{t+x}(t)$, $x \geq 0$. Here, the cross-sectional variable x refers to time-to-maturity. The risk-free asset B is obtained by continuously compounding interest at the prevailing short-term rate $r(t,0)$, *i.e.,* $B(t) = \exp\left(\int_0^t r(u,0)\,du\right)$. Musiela (1993) derives the HJM arbitrage-free interest rate dynamics under the time to maturity parametrization as follows:

$$d_t r(t,x) = \left(\partial_x r(t,x) + \sum_{i=1}^{n} \sigma_i(t,x) \int_0^x \sigma_i(t,u)\,du\right) dt + \sum_{i=1}^{n} \sigma_i(t,x)\,dW_i(t), \qquad (8)$$

starting at $r(0,x) = g(x)$. Here ∂_x denotes partial differentiation with respect to time-to-maturity and g represents the forward rate curve observed at time 0. We require the instantaneous forward rate curve $r(t)$ to be an element in a separable Hilbert space $\mathbb{H}$ endowed with inner product $\langle \cdot, \cdot \rangle_{\mathbb{H}}$ and spanned by a complete orthonormal system $\{f_k\}_{k\in\mathbb{N}}$. We consider the Hilbert space $\mathcal{L}^2_p(\mathbb{R}_+)$ of real-valued functions f defined on the positive real axis such that $\int_0^{+\infty} f(x)^2\, p(x)\,dx < +\infty$. Here $p : \mathbb{R}_+ \to \mathbb{R}_+$ is a suitable function assigning relative weights to different portions of the time-to-maturity spectrum: in the remainder of the paper, we set $p(x) = e^{-\alpha x}$, $\alpha > 0$, so that a greater importance is assigned to short-term than long-term maturities. We consider an evolution equation of the form

$$d_t r(t,x) = \alpha(t,x)\,dt + dW_Q(t,x), \qquad (9)$$

where we take a Brownian motion W_Q in both variables t and x. This process can be represented as the sum of a series

$$W_Q(t,x) := \sum_k \sqrt{\lambda_k(t)} f_k(x)\, W_k(t), \qquad (10)$$

which can be proven to converge whenever $\sum_k \lambda_k(t) < \infty$. In Da Prato and Zabczyk (1992) it is shown that the solution of this equation is the $\mathbb{H}$-valued process

$$r(t,x) = r(0,x) + \int_0^t \alpha(s,x)\,ds + \int_0^t dW_Q(s,x), \qquad \mathbb{P}\text{-a.s.}, \qquad (11)$$

where $r(t,x)$ is an absolutely continuous function in the time-to-maturity variable x. The following result is an extension of equation (8) to dynamics (9).

Theorem 1 (Arbitrage Restriction)[6] Assume the regularity hypotheses stated in Appendix A hold true. Let $\{r(s), 0 \leq s \leq \overline{T}\}$ be an $\mathbb{H} \cap AC(0,\infty)$-valued predictable process satisfying (11). If there are no arbitrage opportunities in the sense of Harrison and Pliska (1981), then

$$\alpha(s,x) = \partial_x r(s,x) + \sum_{k=1}^{\infty} \lambda_k(s) f_k(x) \int_0^x f_k(y)\, dy. \tag{12}$$

Conversely, if $\{\alpha(s), 0 \leq s \leq \overline{T}\}$ is defined by formula (12), then the process $\{r(s), 0 \leq s \leq \overline{T}\}$ indicated by expression (11) defines predictable $\mathbb{H} \cap AC(0,1)$-valued arbitrage-free forward rate dynamics.[7]

Proof. See appendix A. ■

3.3 Discussion

Arbitrage-free forward rate dynamics can be read as:

$$dr(t,x) = \left(\partial_x r(t,x) + \sum_k \lambda_k(t) g_k(x) \right) dt + \sum_k \sqrt{\lambda_k(t)} f_k(x)\, dW_k(t), \tag{13}$$

with $g_k(x) := f_k(x) \int_0^x f_k(y)\, dy$.

From a theoretical perspective, this result shows that infinitely many sources of noise are compatible with the absence of arbitrage opportunities. The resulting drift restriction is fully determined by the market volatility structure with respect to the basis spanning the yield curve space. This result can be extended to non-diagonal covariance structures, leading to arbitrage-free dynamics

$$dr(t,x) = \left[\partial_x r(t,x) + \sum_{k=1}^{\infty} \lambda_k \tau(t,x) f_k(x) \int_0^x \tau(t,y) f_k(y)\, dy \right] dt + \tau(t,x)\, dW_Q(t,x).$$

Notice that this form covers the case of non-linear volatility structures.

[6] This theorem has been independently proved in Guiotto and Roncoroni (1999) and Goldys and Musiela (2001) using different techniques. Our proof is a straight application of the Itô formula for Hilbert space-valued diffusions as reported in Da Prato and Zabczyk (1992).

[7] $AC(0,\infty)$ denotes the class of absolutely continuous functions defined on $[0,\infty)$.

From an operational perspective, the previously cited series expansion provides a representation of the forward rate curve as a superposition of fundamental shapes f_i representing independent sources of risk. Each factor f_j acts as an interpolating or approximating function of the observed rates in the market. Moreover, the relative importance of factor f_j in explaining market risk is measured by a quota λ_i of the overall shape volatility.

When implementing the model, we begin by selecting an orthonormal complete system $\{g_i\}$ for the space H of all forward rate curves. The driving Brownian motion with respect to this basis needs not assume the form (10). In general, it can be represented by:

$$W(t) = \sum b_i(t)\, g_i,$$

where $b_i(t) = \langle W(t), g_i \rangle_{\mathcal{H}}$ are mutually stochastically dependent Brownian motions. The functional version of PCA described in section 2 delivers a basis $\{f_i\}$ under which W has the required form.

The importance of the link we derived between arbitrage free dynamics (13) and factor identification can be appreciated in a variety of contexts. First, we note that extending HJM to countably many Brownian motions may provide a theoretical solution to the incompleteness problem in bond markets. Absence of arbitrage opportunities in this market amounts to imposing a linear constraint across all tradeable bonds. Each constraint defines the following relation between the excess of bond price return over the risk-free asset return $r(t)$ and the bond price volatility:

$$m_T(t) - r(t) = \boldsymbol{\mu}(t) \cdot \mathbf{v}_T(t), \qquad \forall T \geq t. \tag{14}$$

Here m_T and $\mathbf{v}_T$ denote the instantaneous percentage return and, respectively, volatility in the bond price dynamics. Notice that vector $\boldsymbol{\mu}$ represents a time-to-maturity independent market price of risk. It is clear that in a model driven by n Brownian motions this relation holds true up to n degrees of freedom. Heaney and Cheng (1984) note that the number of bonds effectively traded is so much larger than the number of significant noise terms that at least one bond price process does indeed violate the arbitrage constraint (14). The puzzle can be solved by extending the number of independent constraints to infinity. This can be achieved by means of a $\mathcal{Q}$-Brownian motion such as the one we adopt in this paper. Second, it is worth remarking that standard HJM models are usually defined in terms of unobservable state variables. Chiarella and Kwon (2003) remark that expressing state variables in terms of observable quantities may be preferable in several instances. For instance, this occurs

upon modeling term structure volatility functions. Under regularity conditions, the authors suggest simple variable changes transforming arbitrary state variables into functions of bond yields. Shape factors may provide an alternative solution to this problem. Dynamics can be assigned to the shape factors obtained from basic shapes via PCA. In the same line, Collin-Dufresne *et al.* (2008) underline the importance of using state variables that can be easily interpretable and observable before specifying and estimating the model. For a large class of affine structures, they manage to derive a representation in terms of level, slope and convexity of the yield curve at zero. In order to quantify these state variables, a PCA is run to compute a spectral decomposition $\{(\lambda_k, \mathbf{v}_k)\}$, and a yield curve representation around zero:

$$Y(t,x) \approx \sum_{k=1}^{3} \lambda_k(t) f_k(x), \qquad (x \in [0,\varepsilon]) \tag{15}$$

is derived using Taylor expansion. Here the functions $f_k(x)$ on a small right-hand neighborhood $[0,\varepsilon]$ of zero are obtained by implementing a two-step procedure: first, the top four entries of the eigenvectors $\mathbf{v}^1, \mathbf{v}^2$, and $\mathbf{v}^3$ are interpolated using linear, quadratic, and cubic polynomials; second, the resulting functions are extrapolated down to zero. State variables can be obtained by computing $Y(t,0)$ and the partial derivatives $\partial_2 Y(t,0)$ and $\partial_2^2 Y(t,0)$. The method reportedly generates accurate estimates for these figures. However, the choice of interpolating polynomials is somehow arbitrary. The shape factor methodology provides a possible way to select these functions. Let f_k represent the k-th shape factor as defined in expression (6). Then the resulting state variables are compatible to the optimal ranking of interpolating functions in the sense of our functional PCA. At any rate, the adoption of shape factors as interpolating functions may resolve the instability issues noted in Collin-Dufresne *et al.* (2008, p.772, lines 24-27) as a consequence of the local nature of standard PCA.[8] Specifically, computing derivatives on extrapolated curves may lead to an instability effect of the resulting figures as is reported in Rebonato (1998, p.24). Intuitively, a shape factor implementation may resolve this issue by allowing the final user to select an appropriate system of orthonormal functions. In the instance examined by Collin-Dufresne et al. (2008), one calls for using functions exhibiting a stable behavior at zero on a variety of differentiation orders. For our empirical analysis, we instead propose to use exponentially weighed polynomials as a way to stabilize rate (or price) quotes comprised between points

[8]The empirical assessment of the relative quality of these estimates compared to the original ones is beyond the scope of this study which is mainly theoretical.

of interpolation. Besides, a key point in our methodology is that the initial arbitrariness of the selected class of functions goes under an econometric procedure. This latter delivers statistically significant shape factors, whereas extrapolated values obtained using a model free method remain unassessed in their statistical importance.

4 Applications

4.1 Contingent Claims Valuation

Arbitrage-free interest rate models are primarily used for valuation and hedging purposes. Brace and Musiela (1994) and Musiela (1995) derive several formulae for European derivative prices in the Musiela (1993) model driven by a *standard* Brownian motion. We focus on the analytical pricing of European-style interest rate derivatives for interest rate dynamics driven by a $\mathcal{Q}$-Brownian motion W_Q.[9] The basic ingredient required for computing analytic formulae for these securities is the local covariance process of the forward bond yield. By using formulae (26) and (27) reported in appendix B, we may compute the diffusion part of the bond price differential as

$$-P_T\left(s, r\left(s,\cdot\right)\right)\left\langle \frac{\chi_{[0,T-s)}}{p}\left(\cdot\right), dW_Q\left(s,\cdot\right)\right\rangle_{\mathbb{H}}.$$

This expression together with the definition of Q-Brownian motion (see appendix A) allows us to compute the diffusion term of $\log P_T\left(t\right)$ as

$$-\int_0^t \left\langle \frac{\chi_{[0,T-s)}}{p}\left(\cdot\right), \sum_k \sqrt{\lambda_k\left(s\right)} f_k\left(\cdot\right) dW_k\left(s\right)\right\rangle_{\mathbb{H}} = -\int_0^t \sum_k \sqrt{\lambda_k\left(s\right)} \int_0^{T-s} f_k\left(x\right) dx \; dW_k\left(s\right).$$

In particular, the cumulated conditional covariance of the forward bond $P_{T,T_1} := P_{T_1}/P_T$ over a time interval $[t,T]$ is given by

$$\nu^2\left(t,T,T_1\right) := \left\langle \lg \frac{P_{T_1}}{P_T}\right\rangle_T - \left\langle \lg \frac{P_{T_1}}{P_T}\right\rangle_t = \sum_k \int_t^T \lambda_k\left(s\right)\left|\int_{T-s}^{T_1-s} f_k\left(x\right) dx\right|^2 ds. \tag{16}$$

Since term structure dynamics are Gaussian, we can obtain closed-form expressions for European option prices by means of measure change (see Geman *et al.* (1995)).

As a first example, we compute the arbitrage value of a caplet spanning the interval $[T,T_1]$. This is given by:

$$\mathbf{Cpl}^{\nu}_{T,T_1}\left(t\right) = \left(1+\delta K\right)\left(\frac{P_T\left(t, r\left(t\right)\right)}{1+\delta K}\mathcal{N}\left(a_1\right) - P_{T_1}\left(t, r\left(t\right)\right)\mathcal{N}\left(a_2\right)\right), \tag{17}$$

[9] The correspoding PDE formulation is studied in Goldys and Musiela (2001).

where K represents the strike price, $\mathcal{N}$ indicates the cumulative standard normal distribution function, and coefficients a_i are defined by

$$a_1 := \frac{\lg\left(\frac{P_{T_1}(t,r(t))}{P_T(t,r(t))(1+\delta K)}\right)}{\nu(t,T,T_1)} + \frac{\nu(t,T,T_1)}{2}; \quad a_2 := a_1 - \nu(t,T,T_1).$$

As a second example, we evaluate a payer swaption giving the holder the right to enter at a future time T a plain vanilla swap paying out a cash flow stream of fixed amount F at times $T_i = T + i\delta$, for $i = 1, ..., n$. Let $c_k = F\delta$ $(k \neq n)$, $c_n = 1 + F\delta$ and $n(x)$ be the density function of an n-dimensional normal distribution $\mathcal{N}(\mathbf{0}, \mathbf{M})$ with covariance matrix entries

$$M_{ij}(t,T) = \int_t^T \sum_k \lambda_k(s) \left(\int_{T-s}^{T_i-s} f_k(x)\,dx\right)\left(\int_{T-s}^{T_j-s} f_k(x)\,dx\right) ds.$$

The pricing formula for this option is:

$$\mathbf{Swn}^{\nu}_{T,\delta,F}(t) = P_T(t) I^0(t,T) - \sum_{j=1}^{n} c_j P_{T_j}(t) I^j(t,T),$$

where

$$I^j(t,T) = \int_{\mathbb{R}^n} \left(1 - \sum_{k=1}^{n} c_k \frac{P_{T_k}(t)}{P_T(t)} e^{-\frac{\nu^2(t,T,T_k)}{2} - \mathbf{1}_{\mathbb{N}_+}(j) M_{jk}(t) + y_k}\right)_+ n(y_1, ..., y_n)) dy_1 ... dy_n.$$

The same method can be applied to all existing derivative pricing formulae to obtain their analogue in the context of an interest rate model driven by shape factors.

4.2 Cross-Sectional Stability

This section examines a few analytical properties of the shape factor model (13) in view of the cross-sectional consistency introduced in Björk and Christensen (1999). To contextualize our analysis, we briefly recall the issue.

Classes $\mathcal{M}$ of interest rate curve models and $\mathcal{F}$ of terms structures are given. The pair $(\mathcal{M}, \mathcal{F})$ is said to be cross-sectionally consistent in the sense of Björk and Christensen (1999) provided that all realizations of any instance of $\mathcal{M}$ starting at an initial curve in $\mathcal{F}$ is still an element of $\mathcal{F}$. We propose a cross-sectionally consistent pair of an approximately arbitrage-free class of infinite-dimensional dynamics and polynomial class of term structure. This is motivated by the fact that the arbitrage-free dynamics (13) corresponding to a *finite* number of factors coupled with exponentially weighed orthogonal polynomials do not constitute a

cross-sectionally consistent pair. It is widely documented that traders use these polynomials for interpolating market yield curves (see Anderson *et al.*(1996) for a full account).

We therefore proceed as follows. First, we fix a family $\mathcal{F}$ of term structures represented by exponentially weighed orthogonal polynomials; then, we extract an approximately arbitrage-free finite-dimensional system $\mathcal{M}$ from dynamics (13); finally, we prove that $(\mathcal{M}, \mathcal{F})$ is cross-sectionally consistent. The key result in our procedure is that family and model selections are devised in such a way that the pricing errors stemming from the lack of perfect arbitrage freedom by the instances of $\mathcal{M}$ can be exactly measured and minimized at the user's will.

Our approach substantially differs from the alternative strategy followed by La Chioma and Piccoli (2007). These authors consider a finite dimensional Musiela's model and let the family of cross-sections vary in a way that the resulting pair is approximately cross-sectionally consistent. Bayraktar *et al.* (2006) also consider projections of the Musiela's model onto a finite dimensional manifold. However, the problem of measuring the impact of a lack of arbitrage constraints is left unanswered.

Let us consider as given a class $\mathbb{H}$ of interpolating or approximating polynomials and determine term structure dynamics for which the resulting model is cross-sectionally stable and approximately arbitrage-free. We also provide an exact upper bound for the corresponding arbitrage error and show how to make it arbitrarily small. Let arbitrage-free forward rate dynamics be given by the unique mild solution in $\mathbb{H} \cap AC(0,1)$ of equation (13) (Da Prato and Zabczyk (1992)). This process can be written as

$$r(t,x) = e^{t\mathcal{D}} r(0,x) + \sum_k \int_0^t \lambda_k(s)\, e^{(t-s)\mathcal{D}} g_k ds + \sum_k \int_0^t \sqrt{\lambda_k(s)}\, e^{(t-s)\mathcal{D}} f_k dW_k(t), \quad (18)$$

where $\left\{e^{t\mathcal{D}}\right\}_{t\geq 0}$ is the semigroup of translations defined by $\left(e^{t\mathcal{D}}\alpha\right)(x) = \alpha(t+x)$. If the initial term structure $r(0)$ belongs to finite-dimensional space $\mathbb{H}_k :=\text{Span}\{f_1, ..., f_k\}$, then $r(t)$ does not need to be a function in $\mathbb{H}_k$.

Definition 2 (Cross-Sectionally Stable System) The pair $(\mathbb{H}_k, \{r(t), t \geq 0\})$ is said to be a cross-sectionally stable system if $r(0) \in \mathbb{H}_k$ implies that $r(t) \in \mathbb{H}_k$, for all $t \geq 0$.

It is possible to build interest rate dynamics $r(t)$ driven by a finite number of shape factors such that the resulting system $(\mathbb{H}_k, \{r(t), t \geq 0\})$ is cross-sectionally stable. Unfortunately, these dynamics may not be arbitrage-free in the strict sense of Harrison and Pliska (1981). Nevertheless, they are arbitrage-free in the weaker sense specified in the following:

Definition 3 (Quasi Arbitrage-Free Dynamics) Let $r = \{r(t), t \geq 0\}$ be the arbitrage-free dynamics (18). A family $\mathcal{R} = \{r^N, N \in \mathbb{N}\}$ of forward rate dynamics $r^N = \{r^N(t), t \geq 0\}$ is quasi arbitrage-free if for any $\varepsilon > 0$ there exists a number $N_\varepsilon \in \mathbb{N}$ such that

$$\sup_{t \geq 0} \mathbb{E}\left[\left\|r(t) - r^N(t)\right\|_{\mathbb{H}}^2\right] \leq \varepsilon, \quad \forall r_0 \in \mathbb{H}_N, \ \forall N \geq N_\varepsilon.$$

The following proposition provides a quasi arbitrage-free family of cross-sectionally stable systems.

Theorem 2 (Approximation Error) Let the space of all forward rate curves be $\mathbb{H} = \mathcal{L}_p^2(0, +\infty)$ for some smoothing function $p(x) := e^{(2\tau-1)x}$ with $\tau > \frac{1}{2}$ and the subspace of interpolated (or approximated) term structures be $\mathbb{H}_N = \text{Span}\left\{f_0, ..., f_N, \widetilde{f}_0, ..., \widetilde{f}_N\right\}$, where $f_k(x) := L_k(x)e^{-\tau x}$ and $\widetilde{f}_k(x) := L_k(x)e^{-2\tau x}$ are exponentially smoothed Laguerre polynomials. Define the sup-norm:

$$\|r\|_{\infty,[0,T]} := \sup_{t \in [0,T]} \left\|r(t) - r^N(t)\right\|_{\mathbb{H}}. \tag{19}$$

Consider the family $\mathcal{R}$ of forward rate dynamics r^N $(N \in \mathbb{N})$, defined by

$$r^N(t) = e^{t\mathcal{D}} r_0 + \sum_{k=0}^{[\frac{N}{2}]-1} \int_0^t \lambda_k(s) e^{(t-s)\mathcal{D}} g_k \, ds + \sum_{k=0}^{N} \int_0^t \sqrt{\lambda_k(s)} e^{(t-s)\mathcal{D}} f_k \, dW_k(s), \tag{20}$$

where $g_k(x) := f_k(x) \int_0^x f_k(y)\, dy$. Then:

(a) the system $\left(\mathbb{H}_N, r^N\right)$ is cross-sectionally stable, for each $N \in \mathbb{N}$;

(b) the family $\mathcal{R}$ is quasi arbitrage-free. In particular, dynamics $r^N \in \mathcal{R}$ satisfy:

$$\mathbb{E}\left[\left\|r(t) - r^N(t)\right\|_{\mathbb{H}}^2\right] \leq 2\left\{\left[\sum_{k=[\frac{N}{2}]}^{\infty} \int_0^t \lambda_k(s) ds\right]^2 + \sum_{k=N+1}^{\infty} \int_0^t \lambda_k(s) ds\right\}; \tag{21}$$

(c) r^N converges to r in $\mathcal{L}^2(\Omega; \mathcal{C}([0,T]; \mathbb{H}))$ according to the upper bound:

$$\begin{aligned} \mathbb{E}\left[\left\|r(t) - r^N(t)\right\|_{\infty,[0,T]}\right] \ \leq \ & 2\left\{\left[\sum_{k=[\frac{N}{2}]}^{\infty} \int_0^t e^{-(2\tau-1)(T-s)} \lambda_k(s) ds\right]^2 \right. \\ & \left. +4 \sum_{k=N+1}^{\infty} \int_0^t e^{-(2\tau-1)(T-s)} \lambda_k(s) ds\right\} \end{aligned} \tag{22}$$

Proof. See appendix B. ■

This result shows that the approximation error stemming from adopting a cross-sectionally stable system can be made arbitrarily small with respect to the tightest possible norm. This task can be achieved by enlarging the space of basis shapes f_k in a suitable way. Also, the required enlargement depends on the behavior of the sequence of residuals $\left(\int_0^T \lambda_k(s)\,ds\right)_{k\geq N}$. In practical instances, one may select a class $\mathbb{H}_n$ of orthonormal functions, identify the corresponding volatility components λ_k by following the procedure detailed in section 2, and finally assume that any completion of $\mathbb{H}_n$ into a Hilbert space $\mathbb{H}$ brings a negligible contribution to the overall volatility (*i.e.*, the sum of all residuals $\int_0^T \lambda_k ds$ $(k \geq N)$ is negligible in comparison to $\sum_{k=1}^N \int_0^T \lambda_k(s)\,ds$).

The following proposition provides a financial interpretation for the above approximation in terms of mispricing error.

Proposition 3 (Pricing Error) The caplet mispricing error induced by the approximate model (20) satisfies the following upper bound:

$$\mathbb{E}\left[\left|C\left(t,r\left(t\right)\right)-C\left(t,r^N\left(t\right)\right)\right|^2\right] \leq \Lambda_{T_0,T_1}\left\{\left[\sum_{k\geq\left[\frac{N}{2}\right]}\int_0^t \lambda_k(s)\,ds\right]^2+\sum_{k>N}\int_0^t \lambda_k(s)\,ds\right\},$$

for some constant Λ_{T_0,T_1}.

Proof. The caplet price (17) is Lipschitz continuous in $r(t)$. ■

This result, which can be proved for a wider class of interest rate derivatives, justifies the importance of the notion of quasi arbitrage-free families of dynamic interest rate models.

5 Empirical Analysis

We conduct an empirical investigation of cross-sectional risk across a variety of data sets. These include US swap, EUR bond and oil futures markets. Our goal is threefold. First, we examine the ability of shape factors to reproduce the typical movements of cross-sectional data. Second, we measure the extent to which shape factors embody the market risk cumulated over a given period of time. Finally, we assess the relative impact of using an increasing number of shape factors for the pricing of caplets compared to the standard Black quotes. Results indicate that the notion of shape factors plays the double role of "typical curve shift" and "risk source".

5.1 Data

We compute and analyze shape factors on the following three data sets:

- USD swap rates prevailing in the period between March 1, 1988 and February 28, 2002. This data set contains 3653 daily observations, each one collecting *at-par* quoted zero-coupon rates for benchmark times-to-maturity, namely 6 months (x_{6m}), 1 year (x_{1y}), 2 years (x_{2y}), 5 years (x_{5y}), 7 years (x_{7y}), 10 years (x_{10y}), 15 years (x_{15y}), and 20 years (x_{20y}). Maturities correspond to liquid instruments traded in the market under investigation.[10]

- Instantaneous forward rates quoted by ECB over the period between December 29, 2006 and May 22, 2008. Rates are stripped from AAA-rated government bonds in the Euro area and represent 365 daily observations for times-to-maturity equal to 9 months, 1 year, 2 years, 3 years, 4 years, 5 years, 6 years, and 7 years.[11]

- Crude oil futures prices quoted at NYMEX during the period between May 22, 1995 and May 5, 1999. This data set contains 1044 daily observations, each one collecting futures prices for physical delivery of crude oil in four to eleven months.[12]

We consider basis shapes given by smoothed polynomials:

$$\psi_k(x) := L_k(x) \exp(-\tau x), \tag{23}$$

where $L_k(x)$ denotes the Laguerre polynomial of order k and τ is a positive constant.[13] These functions constitute a complete orthonormal system for $\mathcal{L}^2_p[\mathbb{R}^+, \mathbb{R}]$ with respect to a weighting measure with exponential density $p(x) = \exp[(2\tau - 1)x]$, that is

$$\int_0^\infty \psi_k(x)\psi_l(x)e^{(2\tau-1)x}dx = \begin{cases} 1 \text{ if } k = l, \\ 0 \text{ if } k \neq l. \end{cases}$$

Laguerre polynomials ensure adequate flexibility in the interpolation of observed rates, whereas the exponential function guarantees a stable fitting. In this respect, the parameter

[10] Zero-coupon rates correspond to mid-market levels of financial instruments quoted in the market. All rates are determined from a standard "stripping" algorithm assuming linear interpolation. The 6M, the 1Y and 2Y rates are associated with mid-market levels of deposit and LIBOR futures contracts. All remaining zero-coupon rates are obtained from swap rates market quotations. Source: BNP Paribas.

[11] Source: Datastream.

[12] Source: Datastream.

[13] On the use of polynomials for cross-sectional analysis, see Chambers *et al.* (1984).

τ plays a key role in smoothing possible oscillations occurring at the farthest end of the time-to-maturity spectrum where fewer observations are available. Empirical experiments not reported here suggest that τ should be selected between 0.3 and 0.5.[14] The impact of the choice of basis functions is further studied in Galluccio and Roncoroni (2006).

5.2 Test 1: Curve Shapes

Our first test examines the flexibility of the proposed class of basis shapes in fitting daily observed quotes. For each day t, we determine the linear combination of the first eight basis shapes that best fits the observed set of quoted numbers.

Figure 1 about here

Figure 1 exhibits the typical pattern of the first three shape factors extracted from historical data of the three market under concern. Factors one, two, and three are represented by solid, dotted and dashed lines, respectively. In accordance with several empirical studies (*e.g.*, Steeley (1990), Litterman and Scheinkman (1991), D'Ecclesia and Zenios (1994), Barber and Copper (1996), and Bliss (1997), among others), factors corresponding to US data can be interpreted as a parallel shift, a tilt and a bend in the yield curve shape. However, this may not be the case for the other data sets. Figure 1, panel (b), seems to suggest that the main source of risk on Euro bond data is represented by a change in curve slope, while a convexity adjustments rank second and third.[15] Oil price data unveil a third type of market picture. Figure 2, panel (c), shows that parallel shift represents the main contribution to market risk, while convexity adjustments and slope changes rank second and third, respectively.

Overall, shape factor analysis allows a variety of interpretations depending on the actual data under investigation. The common point across all the examined cases is that *exact analytical forms* for rate (or price) curve deformations can be econometrically determined based on market observations. This suggests that shape factors may provide a more reliable cross-rate (resp. cross-price) covariance surface than the one stemming from factors

[14] Our results are quite similar across all values of τ in this range.

[15] In absolute terms, these interpretations may be questioned on the ground of the noticeably low values exhibited on the ordinate axis. However, it is important to note that the graphs are computed on a common scale. This fact allows us to confirm the above claims within the limits of a relative comparison between the two markets under analysis.

resulting from a standard rate (resp. price) based PCA.[16] We explore this point in the next section.

5.3 Test 2: Volatility Recovery

We test the extent to which shape factors can represent the underlying yield curve risk. This kind of risk is commonly measured by the *cross-yield covariance,* namely the empirical covariance matrix of a set of annualized benchmark yield increments over a time period for which reliable market observations are available. The square-root diagonal elements of this matrix define the *yield volatility* function. Litterman and Scheinkman (1991) and Knez *et al.* (1994) identify the yield curve risk factors with the eigenvectors of the cross-yield covariance matrix. A major drawback of this approach is that no information is provided on the risk embodied by yields associated with illiquid maturities. This generates an incorrect assessment of the risk underlying fixed-income positions, and consequently undermines derivatives valuation as well as the corresponding hedging strategies. Because shape factors provide a global representation of yield curve drivers, we argue that a natural measure of yield curve risk is provided by the cross-shape covariance defined in formula (3) of section 2.

We compare cross-yield and cross-shape covariances in terms of their ability to represent the underlying risk using a reduced number of factors. This is accomplished using a two-step analysis. First, we perform PCA's on the cross-yield (or cross-rate, or cross-price) and cross-shape covariance matrices computed on a common data set. Second, we measure the speed at which yield/price and shape risk clusters around uncorrelated factors. This can be done by calculating the percentage of the overall market variance explained by an increasing number of cumulative factors. We refer to the standard factors resulting from traditional PCA of cross-yield, cross-rate, or cross-price covariance matrix as "point factors". The corresponding risk matrix is named "cross-point covariance". This terminology defines a common label for factors computed on yield, rate and price data. It also allow us to underline the local nature of these factors and their volatility assessments compared to our shape factors and the resulting shape volatility curves.

Table 1 reports the results for daily observed Euro rate (1st column) and oil price (2nd column) data. In both cases, shape volatility converges much faster than yield/price volatility. We note that Euro rates movements turn out to experience asynchronous shifts

[16] Standard PCA requires an arbitrary ex-post interpolation of a benchmark set of empirical covariances.

more often than oil prices do on their respective periods of observation. This fact is reflected by the forms displayed by shape factors in the previous section. In terms of volatility clustering, we note that three factors are required to explain the 98% of Euro interest rate risk, whereas two factors suffice to reach the same explicatory power on oil data. A simple inspection of Figure 2 allows us to qualitatively appreciate the rate of convergence of the two quantities.

Figure 2 about here

We extend the previous analysis by exploring the evolution of the convergence rates over time. Table 2 shows the quota α of the overall volatility that is embodied by the most significant one, two, three, and four USD shape and point factors over four distinct periods of time. The first three point factors allow us to capture between 94% and 98% of the total yield volatility, whereas the first three shape factors always account for more than 99% of the observed shape volatility. In all periods, the convergence rate for shape volatility exceeds the one for yield volatility. Moreover, the speed of convergence of shape volatility is rather stable over time, whereas yield volatility convergence exhibits varying speeds across the considered time periods.

We repeat our analysis on weekly observed quotes and check for possible effects stemming from reducing price noise generated by daily monitoring market data. Table 1 reports the resulting figures for oil market data (3rd column). We see that the reduction of spurious noise due to daily observation has a greater impact on the numbers obtained using standard PCA than on those resulting from shape factor analysis. This effect can be explained by the local nature of standard PCA, a property that tends to relatively amplify the negative effect of spurious data noise on the statistical assessment of market risk. The global nature of shape factor analysis allows us to smoothen this noise term on daily observations as well.

We finally remark that cross-yield and cross-shape covariances do not match in general. However, the former can be obtained from the latter by applying formula (7) reported in section 2. We compare yield factors to shape factors in terms of their ability to explain *yield volatility* by a reduced number of risk factors.

Figure 3 about here

Figure 4 about here

Figure 3 (resp., Figure 4) displays US swap and Euro bond yield (resp., oil futures price) volatility functions as obtained by selecting the most representative one, two, three, and

four shape factors (dashed line) and yield (resp., price) factors (plain line). The resulting volatility functions are compared to the historical volatility across a number of times-to-maturity (dots). In summary, the data support the idea that shape factors more accurately model volatility than traditional PCA factors; and, more precisely, that a reduced number of shape factors accounts for the realized rate/price volatility more accurately than the same number of traditional PCA factors. This result confirms the empirical findings in Galluccio and Roncoroni (2006).

5.4 Test 3: Caplet pricing

Our final test aims at measuring the relative impact of the use of shape volatility in pricing interest rate derivatives.

We compute caplet prices using formula (17) under alternative cumulative volatilities:

1. Shape volatility $\nu_3(t, T, T_1)$ recovered using the first three shape factors over the entire US swap data set. This quantity is defined as:

$$\nu_n^2(t, T, T_1) := \sum_{k=1}^{n} \int_t^T \lambda_k(s) \left| \int_{T-s}^{T_1-s} f_k(x)\, dx \right|^2 ds,\ n \geq 1. \tag{24}$$

2. Constant volatility, *i.e.*, the one compatible a traditional Black formula. This figure is calculated as the average three-factor shape volatility over an option maturity ranging from six months to two years and a rate maturity comprised of a value between the caplet maturity and three years later:

$$v_{\text{Black}} := \int_0^3 dx \int_{0.5}^2 dT\ \nu_3(t, T, T+x).$$

Figure 5 about here

Figure 5 exhibits pricing differences along several caplet and underlying rate maturities. We note that price discrepancy increases with options moving towards the deepest out-of-the-money region. As expected, this difference tends to smoothen as long as maturity increases due to the averaging effect displayed in formula (24).

Next, we examine the behavior of price discrepancies as the number of shape factors included in the computation of volatility (24) increases from one to four.

Figure 6 about here

Figure 6 reports a graph of three differences. The surface depicted in Panel (a) represents the difference across varying levels of strike K and option maturity T between the caplet price $\mathbf{Cpl}^{\nu_1}_{T;T_1}(t;T,K)$ computed using one shape factor and the caplet price $\mathbf{Cpl}^{\nu_2}_{T,T_1}(t;T,K)$ computed using two shape factors. The surfaces exhibited in Panel (b) and Panel (c) display similar figures for the cases involving three and four shape factors, respectively. We clearly see the price discrepancies primarily affect the long-run out-of-the-money region.

6 Conclusions

Based on empirical findings reported in Galluccio and Roncoroni (2006) about the ability of cross-sectional data to provide relevant information on dynamic risk in fixed income markets, we put forward a theoretically sound measure of risk accounting for an explicit link between cross-sectional shapes and market volatility. We develop a continuous-time infinite-dimensional arbitrage-free model for interest rate dynamics driven by shape factors representing the aforementioned kind of risk. A number of applications are presented and, overall, our analysis provides a theoretical ground and an additional empirical confirmation of the quality of shape factors to represent cross-sectional risk.

Shape factor modeling opens a wide range of possible developments. We envisage three possible directions for future research. First, an additional assessment of the hedging performance of shape factor models with respect to standard factor models across alternative markets. Second, the numerical evaluation of complex derivatives through "shape-valued lattices" and the development of a corresponding weak convergence theory. Finally, the design of estimation procedures for time-varying, and possibly stochastic shape volatility models.

A Appendix: Proof of Theorem 1

Under regularity conditions on the bond price volatilities, the discounted bond process $\frac{P_T(t)}{B(t)}$is a martingale if its drift vanishes. By Itô formula for $\mathbb{H}$-valued processes:,

$$\frac{P_T(t,r(t))}{B(t)} = P_T(0,r(0)) - \int_0^t P_T(s,r(s))\, B(s)^{-1} r(s,0)\, ds + \int_0^t B(s)^{-1} d_s P_T(s,r(s)), \tag{25}$$

$$\begin{aligned} P_T(t,r(t)) &= P_T(0,r(0,\cdot)) + \int_0^t \{\partial_s P_T(s,r(s)) + \langle \partial_r P_T(s,r(s)), \alpha(s)\rangle_{\mathbb{H}} \\ &\quad + \frac{1}{2}\mathrm{Tr}\left[\partial^2_{rr} P_T(s,r(s)) \sqrt{Q(s)} \left(\sqrt{Q(s)}\right)^*\right]\Big\} ds + \int_0^t \langle \partial_r P_T(s,r(s)), dW_Q(s)\rangle_{\mathbb{H}}. \end{aligned} \tag{26}$$

Here * indicates the corresponding adjoint operator. The relevant partial derivatives of the bond price are given by

$$\partial_s P_T(s,r)\,|_{r=r(s)} = P_T(s,r(s))\, r(s,T-s), \tag{27}$$

$$\partial_r P_T(s,r)\,|_{r=r(s)} = -P_T(s,r(s)) \frac{\chi_{[0,T-t)}}{p}(\cdot) \in \mathbb{H}, \tag{28}$$

$$\partial^2_{rr}\, P_T(s,r)|_{r=r(s)} = P_T(s,r(s)) \left(\frac{\chi_{[0,T-t)}}{p}(\cdot) \otimes \frac{\chi_{[0,T-t)}}{p}(\cdot)\right) \in L(\mathbb{H}), \tag{29}$$

where $\frac{\chi_{[0,T-t)}}{p}$ is defined by $\frac{\chi_{[0,T-t)}}{p}(x) := \chi_{[0,T-t)}(x)/p(x)$. Formula (27) is trivial. Formula (28) stems form the fact that

$$\lg P_T(t,r(t)+h) - \lg P_T(t,r(t)) = \int_0^{T-t} h(x)\, dx = \left\langle \frac{\chi_{[0,T-t)}}{p}(\cdot), h(\cdot)\right\rangle_{\mathbb{H}}.$$

Formula (29) is obtained by using the first order approximation of the increment in the first order derivative $\partial_r P_T$ as computed by

$$\begin{aligned} \partial_r P_T(t,r(t)+h) - \partial_r P_T(t,r(t)+h) &= -P_T(t,r(t)+h)\frac{\chi_{[0,T-t)}}{p} + P_T(t,r(t))\frac{\chi_{[0,T-t)}}{p} \\ &= P_T(t,r(t))\frac{\chi_{[0,T-t)}}{p}(\cdot)\left(-e^{-\int_0^{T-t} h(u)du} + 1\right) \\ &\simeq P^T(t,r(t))\,\chi_{[0,T-t)}(\cdot)\int_0^{T-t} h(u)\, du \\ &= P^T(t,r(t))\left(\frac{\chi_{[0,T-t)}}{p} \otimes \frac{\chi_{[0,T-t)}}{p}\right)(h(\cdot)) \end{aligned}$$

Substituting formulae (27), (28) and (29) into expression (26), the drift of the discounted bond price vanishes if and only if

$$\begin{aligned} 0 &= -r(s,0) + r(s,T-s) - \left\langle \frac{\chi_{[0,T-s)}}{p}(\cdot), \alpha(s) \right\rangle_{\mathbb{H}} \\ &\quad + \frac{1}{2}\mathrm{Tr}\left[\left(\frac{\chi_{[0,T-s)}}{p} \otimes \frac{\chi_{[0,T-s)}}{p} \right) \sqrt{Q(s)} \left(\sqrt{Q(s)} \right)^* \right]. \end{aligned} \tag{30}$$

This condition needs to hold on the whole time horizon. The trace in formula (26) is given by

$$\sum_{k=1}^{\infty} \left\langle \left(\frac{\chi_{[0,T-s)}}{p} \otimes \frac{\chi_{[0,T-s)}}{p} \right) \sqrt{Q(s)} f_k, \sqrt{Q(s)} f_k \right\rangle_{\mathbb{H}} = \sum_{k=1}^{\infty} \lambda_k(s) \left(\int_0^{T-s} f_k(y)\, dy \right)^2,$$

and setting $x = T - s$, one obtains:

$$0 = -r(s,0) + r(s,x) - \int_0^x \alpha(s,y)\, dy + \frac{1}{2} \sum_{k=1}^{\infty} \lambda_k(s) \left(\int_0^x f_k(y)\, dy \right)^2, \tag{31}$$

for every $x \geq 0$ and $s \geq 0$. By taking partial derivatives with respect to x in this expression, we obtain the required drift restriction. ■

B Appendix : Proof of Theorem 2

The proof is split into two parts. **Part (a)** - Let $r_0 \in \mathbb{H}_N$. An inspection of (20) shows that $r^N \in \mathbb{H}_N$ whenever the three involved summands do. For this, we need to show that: (1) functions $f_k, k = 0, ..., N$ belong to $\mathbb{H}_N$, (2) functions $g_k, k = 0, ..., \left[\frac{N}{2}\right] - 1$ belong to $\mathbb{H}_N$, and (3) the shift operator $e^{t\mathcal{D}}$ does not bring out of $\mathbb{H}_N$, *i.e.*, $e^{t\mathcal{D}}\mathbb{H}_N \subset \mathbb{H}_N$. The first statement follows from the very definition of $\mathbb{H}_N$. As for the second statement, notice that each integral g_k is a linear combinations of functions $f_k \times f_j$, for $j = 0, \ldots, k$. Indeed:

$$\int_0^x e^{-\tau y} L_k(y)\ dy = \sum_{j=0}^{k} \frac{1}{\tau^{j+1}} L_k^{(j)}(0) - \sum_{j=0}^{k} \frac{1}{\tau^{j+1}} e^{-\tau x} L_k^{(j)}(x)$$

and $L_k^{(j)}$ is a polynomial of degree $k - j$, so that each function: $x \mapsto \int_0^x f_k(y)\ dy$ is an element in $\mathrm{Span}\{f_1, \ldots, f_k\}$. Now, each function $f_k \times f_j$ can be written as

$$f_k(x) f_j(x) = e^{-\tau x} L_k(x) e^{-\tau x} L_j(x) = e^{-2\tau} p_{k+j}(x),$$

where p_{k+j} is a polynomial of degree no greater than $k+j \leq 2k$. In particular, p_{k+j} can be represented as a linear combination of polynomials $L_0, \ldots, L_{2k}$. Consequently, each function $f_k \times f_j$ is in $\text{Span}\left\{\widetilde{f}_0, \ldots \widetilde{f}_{2k}\right\}$. Therefore $g_k \in \mathbb{H}_N$ whenever $k \leq \left[\frac{N}{2}\right] - 1$. To prove the third statement, notice that translating function f_k leads to

$$e^{t\mathcal{D}} f_k(x) = L_k(x+t)e^{-\tau(x+t)} = e^{-\tau t}e^{-\tau x} p_k^{(t)}(x),$$

where $p_k^{(t)}(x)$ is a polynomial of degree k in x with coefficients depending on t. Clearly, $p_k^{(t)}(x)$ can be represented as a linear combination of $L_1, \ldots, L_k$ with time-dependent coefficients, *i.e.,* $p_k^{(t)} = \sum_{j=1}^{k} a_j(t) L_j(x)$. Thus, $e^{t\mathcal{D}} f_k$ is a linear combination of functions $e^{-\tau x} L_j(x)$, $j = 1, \ldots, k$, with time-dependent coefficients, *i.e.,* $e^{t\mathcal{D}} f_k(x) \in \mathbb{H}_k \subset \mathbb{H}_N$.

Part (b) - By definitions (18) and (20) we have:

$$\begin{aligned} \left\| r\left(t\right) - r^N\left(t\right) \right\|_{\mathbb{H}}^2 \quad \leq \quad & 2\left\{ \left[\sum_{k=\left[\frac{N}{2}\right]}^{\infty} \int_0^t \lambda_k(s) \left\| e^{(t-s)\mathcal{D}} g_k \right\|_{\mathbb{H}} ds \right]^2 \right. \\ & \left. + \left\| \sum_{k=N+1}^{\infty} \int_0^t \sqrt{\lambda_k\left(s\right)} e^{(t-s)\mathcal{D}} f_k dW_k\left(s\right) \right\|_{\mathbb{H}}^2 \right\}. \end{aligned} \tag{32}$$

Let us focus on the first summand. Since

$$\|e^{t\mathcal{D}} f\|_{\mathbb{H}}^2 = \int_0^{+\infty} f(x+t)^2 p(x)\, dx = \int_t^{+\infty} f(y)^2 p(y-t)\, dy \leq e^{-(2\tau-1)t} \|f\|_{\mathbb{H}}^2,$$

we obtain an upper bound $\|e^{(t-s)\mathcal{D}} g_k\|_{\mathbb{H}} \leq e^{-(2\tau-1)(t-s)} \|g_k\|_{\mathbb{H}}$. Moreover

$$\|g_k\|_{\mathbb{H}}^2 = \int_0^{\infty} g_k(x)^2 p(x)\, dx = \int_0^{\infty} f_k(x)^2 \left(\int_0^x f_k(y)\, dy \right)^2 p(x)\, dx,$$

and the Hölder inequality gives

$$\begin{aligned} \left(\int_0^x f_k(y)\, dy \right)^2 \quad &= \quad \left(\int_0^x f_k(y) \sqrt{p(y)} \sqrt{p(-y)}\, dy \right)^2 \\ &\leq \quad \int_0^x f_k(y)^2 p(y)\, dy \int_0^x p(-y)\, dy \\ &\leq \quad \|f_k\|_{\mathbb{H}}^2 \frac{1 - e^{-(2\tau-1)x}}{2\tau - 1} \leq 1. \end{aligned}$$

Hence, $\|g_k\|_{\mathbb{H}} \leq \|f_k\|_{\mathbb{H}} \leq 1$, for all $k \geq 0$, and the first summand in (32) is superiorly bounded by $\sum_{k=\left[\frac{N}{2}\right]}^{\infty} \int_0^t \lambda_k(s)\, ds$. As for the second summand in (32), taking expectation

and using the stochastic version of Fubini theorem, we obtain an upper bound:

$$\begin{aligned}
&\mathbb{E}\left[\left\|\sum_{k=N+1}^{\infty}\int_0^t \sqrt{\lambda_k(s)}e^{(t-s)\mathcal{D}}f_k dW_k(s)\right\|_{\mathbb{H}}^2\right] \\
&\leq \sum_{k=N+1}^{\infty}\mathbb{E}\left[\left\|\int_0^t \sqrt{\lambda_k(s)}e^{(t-s)\mathcal{D}}f_k dW_k(s)\right\|_{\mathbb{H}}^2\right] \\
&= \sum_{k=N+1}^{\infty}\int_0^t \lambda_k(s)\left\|e^{(t-s)\mathcal{D}}f_k\right\|_{\mathbb{H}}^2 ds \leq \sum_{k=N+1}^{\infty}\int_0^t \lambda_k(s)\, ds.
\end{aligned}$$

This proves expression (21). This bound together with the assumption $\sum_k \lambda_k(t) < \infty$ proves that $\mathcal{R}$ is quasi-arbitrage-free.

Part (c) - Similarly to part (b), we notice that:

$$\begin{aligned}
\left\|r(t) - r^N(t)\right\|_{\mathbb{H}}^2 \leq\ & 2\left\{\left\|\sum_{k=\left[\frac{N}{2}\right]}^{\infty}\int_0^t \lambda_k(s)e^{(t-s)\mathcal{D}}g_k\, ds\right\|_{\mathbb{H}}^2\right. \\
&\left.+\left\|\sum_{k=N+1}^{\infty}\int_0^t \sqrt{\lambda_k(s)}e^{(t-s)\mathcal{D}}f_k dW_k(s)\right\|_{\mathbb{H}}^2\right\}.
\end{aligned} \tag{33}$$

As long as $\left\|e^{t\mathcal{D}}\right\|_{\mathbb{H}}^2 \leq e^{-(2\tau-1)t}$, the expected supremum of the first summand is upperly bounded by:

$$\mathbb{E}\left[\sup_{t\in[0,T]}\sum_{k=\left[\frac{N}{2}\right]}^{\infty}\int_0^t \lambda_k(s)\left\|e^{(t-s)\mathcal{D}}g_k\right\|_{\mathbb{H}}^2\right] ds \leq \sum_{k=\left[\frac{N}{2}\right]}^{\infty}\int_0^T e^{-(2\tau-1)(t-s)}\lambda_k(s)\, ds. \tag{34}$$

For the second summand, $M_N(t) := \sum_{k=N+1}^{\infty}\int_0^t \sqrt{\lambda_k(s)}e^{(t-s)\mathcal{D}}f_k dW_k(s)$ is a $\mathbb{P}^*$-martingale under its natural filtration. Using Doob inequality and Itô isometry, we have:

$$\begin{aligned}
\mathbb{E}\left[\left(\sup_{t\in[0,.T]}\|M_N(t)\|_{\mathbb{H}}\right)^2\right] &\leq 4\mathbb{E}\left[\|M_N(T)\|_{\mathbb{H}}^2\right] \\
&\leq 4\sum_{k=N+1}^{\infty}\mathbb{E}\left[\left\|\int_0^T \sqrt{\lambda_k(s)}e^{(T-s)\mathcal{D}}f_k dW_k(s)\right\|_{\mathbb{H}}^2\right] \\
&\leq 4\sum_{k=N+1}^{\infty}\int_0^T e^{-(2\tau-1)(T-s)}\lambda_k(s)\, ds.
\end{aligned}$$

This bound combined with (34) into expression (33) leads to the claimed inequality (22). Consequently r^N converges to r in $\mathcal{L}^2(\Omega;\mathcal{C}([0,T];\mathbb{H}))$. ■

References

Aihara, S.I., and A. Baghi. "Stochastic Hyperbolic Dynamics for Infinite-Dimensional Forward Rates and Option Pricing." Mathematical Finance, 15(1) (2005) 27-47.

Anderson, N., F. Breedon, M. Deacon, A. Derry, and G. Murphy. Estimating and Interpreting the Yield Curve, John Wiley & Sons, New York (1996).

Barber, J.R., and M.L. Copper. "Immunization Using Principal Components Analysis." Journal of Portfolio Management, Summer (1996), 99-105.

Barrett, W.B., T.F. Gosnell Jr., and A.J. Heuson. "Yield Curve Shifts and the Selection of Immunization Strategies." Journal of Fixed Income, September (1995), 53-64.

Bayraktar, E., L. Chen, and H.V. Poor. "Projecting the Forward Rate Flow onto a Finite Dimensional Manifold." International Journal of Theoretical and Applied Finance, 9(5) (2006), 777–785.

Björk, T., and B.J. Christensen. "Interest Rate Dynamics and Consistent Forward Rate Curves." Mathematical Finance, 9 (1999), 323-348.

Bliss, R. R. "Movements on the Term Structure of Interest Rates." Economic Review, Federal Reserve Bank of Atlanta, Fourth quarter (1997), 16-33.

Bouchaud, J.-P., N. El Karoui, R. Cont, M. Potters, and N. Sagna. "Phenomenology of the Interest Rate Curve." Applied Mathematical Finance 6 (1999), 209-232.

Brace, A., and M. Musiela. "A Multifactor Gauss-Markov Implementation of Heath, Jarrow and Morton." Mathematical Finance, 3 (1994), 259-283.

Chambers, D.R., and W.T. Carleton. "A Generalized Approach to Duration." In Research in Finance, A.H. Chen, Ed. Greenwich, CT, JAI Press (1988), 163-181.

Chiarella, C., O.K. Kwon. "Finite Dimensional Affine Realizations of HJM Models in Terms of Forward Rates and Yields." Review of Derivatives Research 6 (2003), 129-155.

Collin-Dufresne, P., and R.S. Goldstein. "Generalizing the Affine Framework to HJM and Random Field Models." Working Paper, Carnegie Mellon University (2003).

Collin-Dufresne, P., Goldstein, R.S., and C.S. Jones. "Identification of Maximal Affine Term Structure Models." The Journal of Finance, 63(2) (2008), 743-795.

Cox, J.C., Ingersoll, J.E., and S.A. Ross. "A Theory of the Term Structure of Interest Rates." Econometrica, 53 (1985), 385-408.

Da Prato, G., and J. Zabczyk. Stochastic Equations in Infinite Dimensions, Cambridge University Press, Cambridge (1992).

D'Ecclesia, R.L., and S.A. Zenios. "Risk Factor Analysis and Portfolio Immunization in the Italian Bond Market." Journal of Fixed Income, September (1994), 51-58.

Elton, E.J., Gruber, M.J., and R. Michaely. "The Structure of Spot Rates and Immunization." The Journal of Finance, 45 (1990), 629-642.

Engle, R.F., and V.K. Ng. "Time-Varying Volatility and the Dynamic Behavior of the Term Structure." Journal of Money, Credit and Banking 25-3 (1993), 336-349.

Filipović, D. "Consistency Problems for HJM Interest Rate Models", Ph.D. Dissertation, ETH Zurich (2000).

Fisher, E.O., and R. Weil. "Coping with the Risk of Interest Rate Fluctuations: Returns to Bond Holders from Naive and Optimal Strategies." Journal of Business, 44 (1972).

Fong, H.G., and O.A. Vasiček. "A Risk Minimizing Strategy for Portfolio Immunization." Journal of Finance, 39 (1984), 1541-1546.

Galluccio, S., and A. Roncoroni. "A New Measure of Cross-Sectional Risk and its Empirical Implications on Portfolio Risk Management" Journal of Banking and Finance, 30 (2006), 2387-2408.

Geman, H., N. El Karoui, and C. Rochet. "Changes of Numéraire, Changes of Probability Measures and Option Pricing." Journal of Applied Probability 32 (1995), 443-458.

Goldys, B., and M. Musiela. "Infinite Dimensional Diffusions, Kolmogorov Equations and Interest Rate Models." In: Handbooks in Mathematical Finance: Option Pricing, Interest Rates and Risk Management, E. Jouini, J. Cvitanic, and Musiela. Eds., Cambridge University Press (2001), 314-335.

Goldstein, R.S. "The Term Structure of Interest Rates as a Random Field." Review of Financial Studies, 13-2 (2000), 365-384.

Guiotto, P, and A. Roncoroni. "Infinite Dimensional HJM Dynamics for the Term Structure of Interest Rates." Working Paper 9903, ESSEC (1999).

Harrison, R.J., and S. Pliska. "Martingales and Stochastic Integrals in the Theory of Continuous Trading." Stochastic Processes and Their Applications, 11 (1981), 215-260.

Heath, D., R. Jarrow, and A. Morton. "Bond Pricing and the Term Structure of Interest Rates: A New Methodology." Econometrica, 61 (1992), 77-105.

Heaney, W.J., and P.L. Cheng. "Continuous Maturity Diversification of Default-Free Portfolios and a Generalization of Efficient Diversification." Journal of Finance, 39 (1984), 1101-1117.

Kennedy, D. "The Term Structure of Interest Rates as a Gaussian Random Field." Mathematical Finance, 4 (1994), 247-258.

Kennedy, D. "Characterizing Gaussian Models of the Term Structure of Interest Rates." Mathematical Finance, 7 (1997), 107-118.

Kimmel, R.L. "Modeling the Term Structure of Interest Rates: A New Approach." Journal of Financial Economics, 72 (2004), 143-183.

Knez, P.J., R. Litterman, and J. Scheinkman. "Explorations Into Factors Explaining Money Market Returns." Journal of Finance, 5 (1994), 1861-1882.

La Chioma, C., and B. Piccoli. "Heath-Jarrow-Morton Interest Rate Dynamics and Approximately Consistent Forward Rate Curves." Mathematical Finance, 17(3) (2007), 427–447.

Litterman, R., and J. Scheinkman. "Common Factors Affecting Bond Returns." Journal of Fixed Income, 1 (1991), 54-61.

Litterman, R., J. Scheinkman, and L. Weiss. "Volatility and the Yield Curve." Journal of Fixed Income 1 (1991), 49-53.

Musiela, M. "Stochastic PDEs and Term Structure Models." Journées Internationales de Finance, IGR-AFFI. La Baule (1993).

Musiela, M. "General Framework for Pricing Derivative Securities." Stochastic Processes and their Applications, 55 (1995), 227-251

Nelson, C.R, and A.F. Siegel. "Parsimonious Modelling of Yield Curves." Journal of Business, 60(4) (1987), 473-489.

Pang, K. "Calibration of Gaussian Heath, Jarrow and Morton and Random Field Interest Rate Term Structure Models." Review of Derivatives Research, 2 (1999), 315-345.

Phoa, W., and M. Shearer. "A Note on Arbitrary Yield Curve Reshaping Sensitivities Using Key Rate Durations." Journal of Fixed Income, December (1997), 67-71.

Prisman, E.Z., and M.R. Shores. "Duration Measures for Specific Term Structure Estimations and Applications to Bond Portfolio Immunization." Journal of Banking and Finance, 12 (1988), 493-504.

Rebonato, R. Interest-Rate Option Models. Wiley & Sons, London (1998).

Rodrigues de Almeida, C. I., A.M. Duarte Jr, and C.A. Coelho Fernandes. "Decomposing and Simulating the Movements of Term Structures of Interest Rates in Emerging Eurobond Markets." Journal of Fixed Income, June (1998), 21-31.

Santa Clara, P., and D. Sornette. "The Dynamics of the Forward Interest Rate Curve as a Stochastic String Shock." Review of Financial Studies, 14 (2001), 149-185.

Steeley, J.M. "Modelling the Dynamics of the Term Structure of Interest Rates." Economic and Social Review, 21 (1990), 337-361.

Walsh, J.B. "An Introduction to Stochastic Partial Differential Equations." In Ecole d'Eté de Probabilité de Saint-Flour, Lecture Notes in Mathematics, 1180, Springer-Verlag, Berlin (1986).

	Eurobond (daily)		Oil (daily)		Oil (weekly)	
Factor N$^{\circ}$	Shape	Yield-based	Shape	Price-based	Shape	Price-based
1	85.16	52.24	93.66	85.80	93.2127	77.8008
1+2	94.76	76.58	98.25	95.04	97.3659	91.3693
1+2+3	98.88	88.16	100.00	96.85	100.00	94.6888
1+2+3+4	99.63	92.23	100.00	97.88	100.00	96.4315

Table 1: Percentage quota of the overall shape and yield (resp. oil price) volatility that is embodied by the most significant one, two, three, and four shape and yield (resp. oil price) factors over the period between December 29, 2006 and May 22, 2008 (resp. May 22, 1995 and May 5, 1999). Figures refer to daily recorded Eurobond yields quoted by ECB (resp. daily and weekly recorded crude oil futures prices quoted at NYMEX) over the reference period (Source: Datastream).

	March, 1st 88-91		March, 1st 91-94		March, 1st 94-97		March, 1st 97-02	
Factor N$^{\circ}$	Shape	Yield	Shape	Yield	Shape	Yield	Shape	Yield
1	78.76	78.09	77.19	76.48	82.47	91.03	81.29	86.07
1+2	97.11	92.58	95.37	90.65	97.29	97.74	97.36	97.22
1+2+3	99.14	96.35	99.02	94.64	99.56	98.95	99.52	98.83
1+2+3+4	99.83	98.05	99.68	96.58	99.95	99.50	99.96	99.44

Table 2: Percentage quota of the overall shape (resp. yield) volatility that is embodied by the most significant one, two, three, and four shape (resp. point) factors over four distinct periods of time. Figures refer to daily monitored USD swap market quotes prevailing in reported subperiods between March 1, 1988 and February 28, 2002 (Source: BNP Paribas).

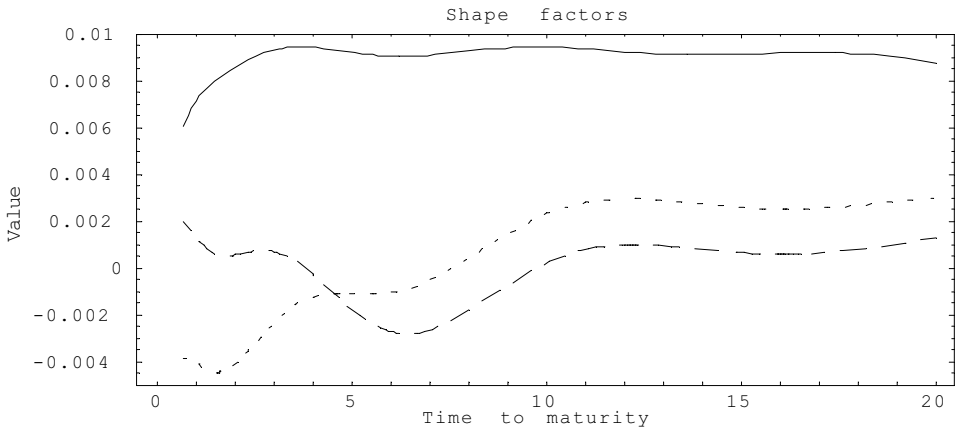

(a)

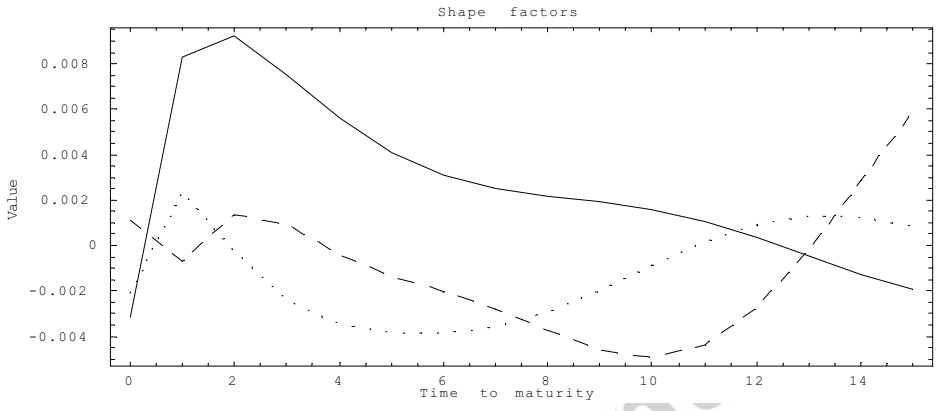

(b)

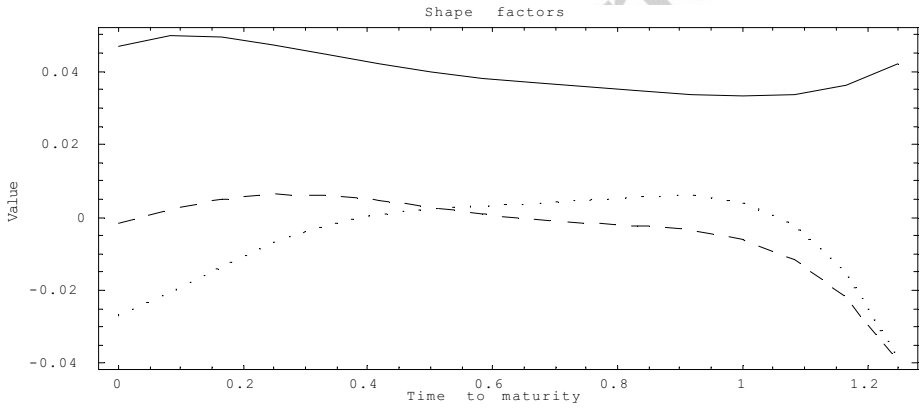

(c)

Figure 1. Panel (a): First three shape factors in the USD swap market prevailing in the period between March 1, 1988 and February 28, 2002 (Source: BNP Paribas). This data set contains 3653 daily observations, each one collecting *par* zero-coupon rates for benchmark times-to-maturity corresponding to 6 months, 1 year, 2 years, 5 years, 7 years, 10 years, 15 years, and 20 years. The first shape factor (solid line) represents a parallel shift; the second shape factor (dotted line) drives variation in slope; the third shape factor (dashed line) embodies a convexity adjustment.
Panel (b) First three shape factors in the Eurobond markets prevailing in the period between December 29, 2006 and May 22, 2008 (Source: DataStream). This data set contains 365 daily observations of instantaneous forward rates quoted by the European Central Bank (ECB). Rates are stripped from AAA-rated government bonds in the Euro area and refer to times-to-maturity equal to 9 months, 1 year, 2 years, 3 years, 4 years, 5 years, 6 years, and 7 years. The first shape factor (solid line) represents a change in curve slope; the second and the third shape factors (dotted and dashed lines, respectively) drive convexity adjustments.
Panel (c) First three shape factors in the oil futures markets prevailing in the period between May 22, 1995 and May 5, 1999 (Source: DataStream). This data set contains 1044 daily observations of futures prices quoted at NYMEX for physical delivery of crude oil in four to eleven months at a monthly pace. The first shape factor (solid line) represents a parallel shift; the second shape factor (dotted line) embodies a convexity adjustment; the third shape factor (dashed line) drives variation in curve slope.

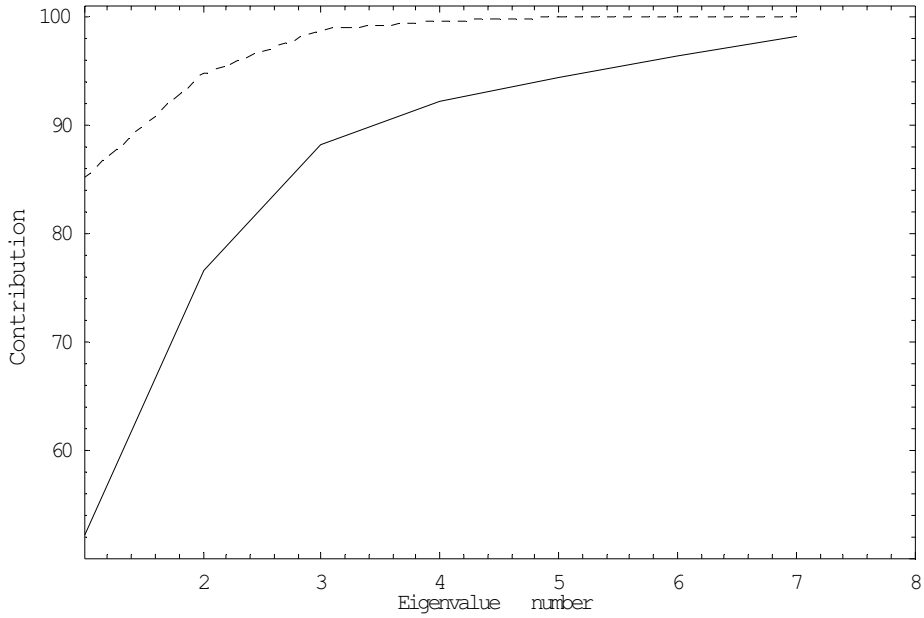

(a)

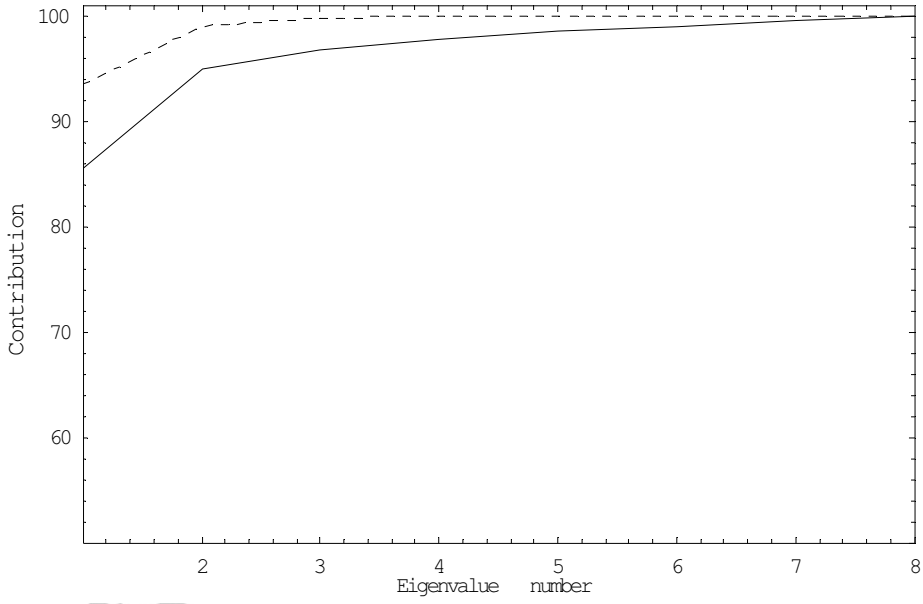

(b)

Figure 2. Panel (a): Percentage contribution to the recovery of Euro bond shape volatility (dashed line) and yield volatility (solid line) for an increasing number of retained most significant factors. Figures are derived from Eurobond market ECB quotes prevailing in the period between December 29, 2006 and May 22, 2008 (Source: DataStream).
Panel (b): Percentage contribution to the recovery of crude oil futures shape volatility (dashed line) and price volatility (solid line) for an increasing number of retained most significant factors. Figures are derived from crude oil future quotes prevailing in the period between May 22, 1995 and May 5, 1999 at NYMEX (Source: DataStream).

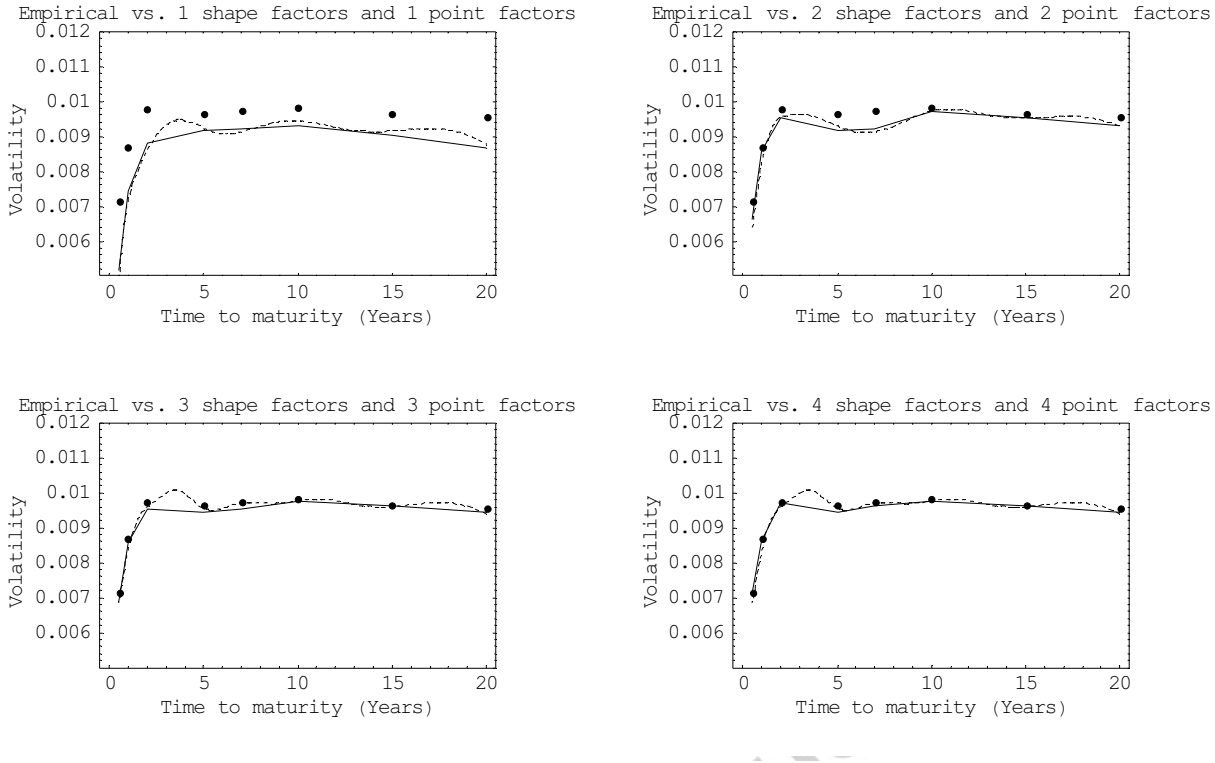

(a)

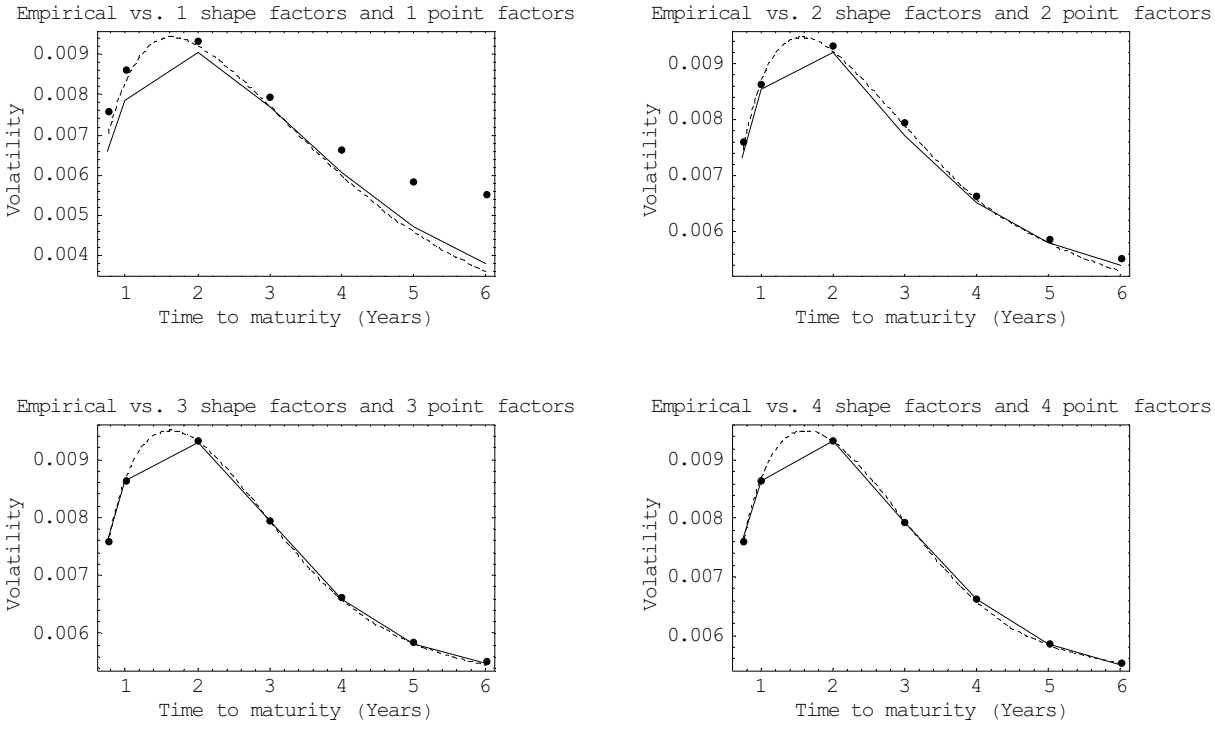

(b)

Figure 3: Historical volatilities computed at benchmark times-to-maturity (dots) *vs*. volatility curve recovered using the first one, two, three, and four more significant yield factors (plain line) and shape factors (dashed line).
Panel (a) refers to USD swap market quotes prevailing in the period between March 1, 1988 and February 28, 2002 (Source: BNP Paribas);
Panel (b) refers to ECB quoted Eurobond yields prevailing in the period between December 29, 2006 and May 22, 2008 (Source: DataStream).

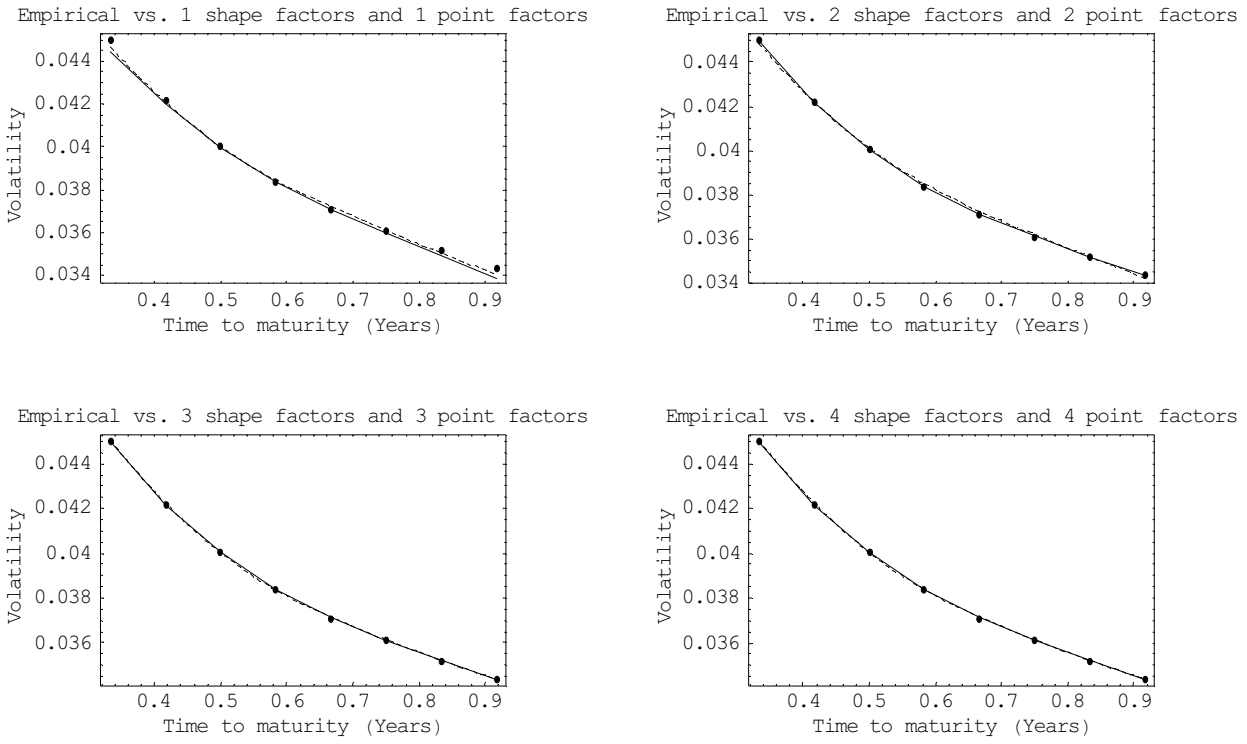

Figure 4: Historical volatilities computed at benchmark times-to-maturity (dots) *vs*. volatility curve recovered using the first one, two, three, and four more significant price factors (plain line) and shape factors (dashed line). Figures refer to oil futures market quotes prevailing in the period between May 22, 1995 and May 5, 1999 (Source: DataStream).

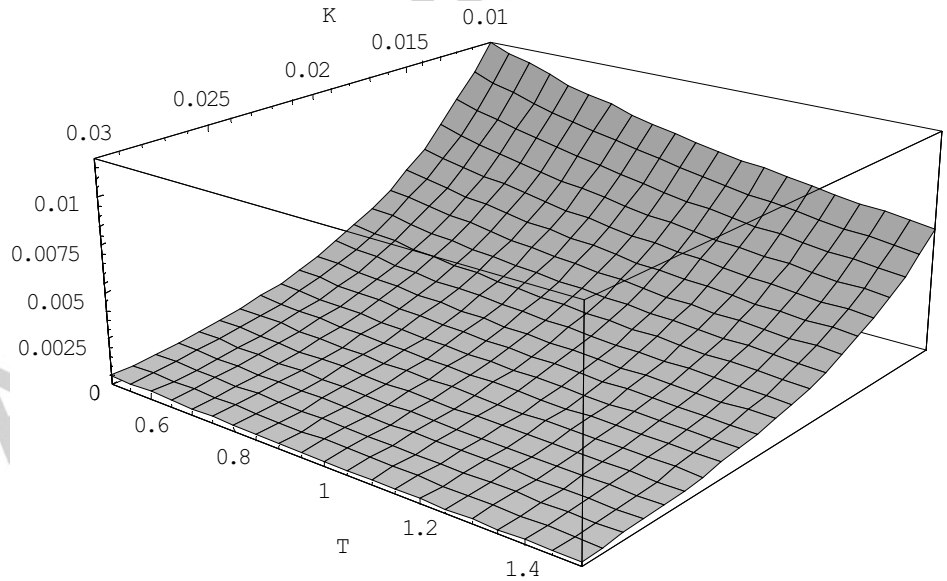

Figure 5: Caplet price excess of fair value computed using shape volatility over fair value computed using constant Black volatility across varying times-to-maturity and strikes. Shape volatility is recovered using the first three most significant shape factors over the entire data set. Constant Black volatility is calculated as the average shape volatility over option maturities ranging from six months to two years and rate maturities comprised between the caplet maturity and three years later. Figures refer to USD swap market quotes prevailing in the period between March 1, 1988 and February 28, 2002 (Source: BNP Paribas)

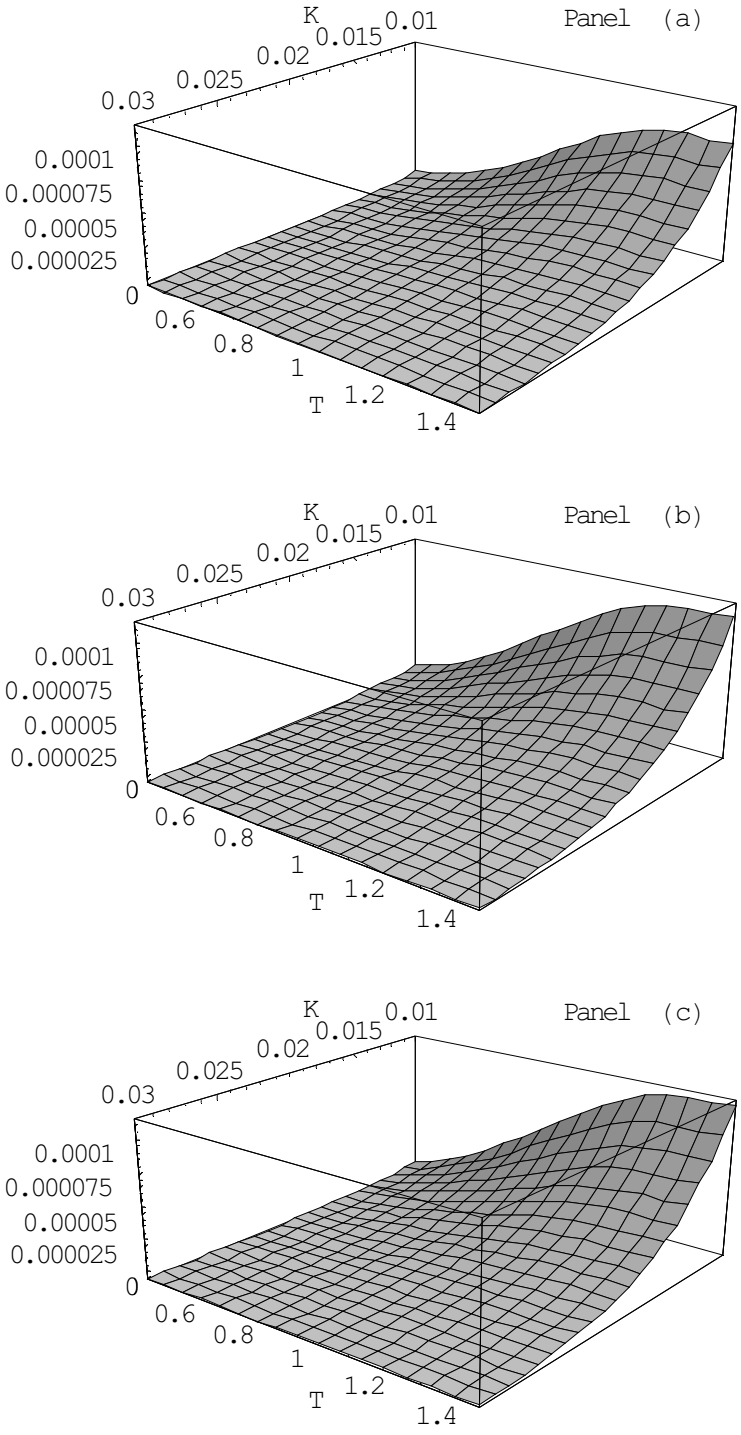

Figure 6: Divergence of caplet prices computed using shape volatility recovered using an increasing number of retained shape factors. Panel (a) represents the difference across varying levels of strike K and option maturity T between the caplet price computed using one shape factor and the caplet price computed using two shape factors. The surfaces exhibited in Panel (b) and Panel (c) display similar figures for the cases involving three and four shape factors, respectively. Figures refer to USD swap market quotes prevailing in the period between March 1, 1988 and February 28, 2002 (Source: BNP Paribas).